ANALYSIS OF LOFT TEST L3-6

PERFORMED BY

COMBUSTION ENGINEERING, INC.

APRIL 1, 1981

ABSTRACT

This report presents a best-estimate blind analysis and a best-estimate post-test analysis of LOFT Test L3-6 performed by Combustion Engineering, Inc. for the C-E Owner's Group on Post-TMI Efforts.

LOFT Test L3-6 was the sixth experiment in the LOFT Small Break Series and simulated a 0.1 ft^2 communicative break at the pump discharge of a large PWR. L3-6 differed from previous LOFT Small Break Tests in that the pumps remained powered throughout the test.

The analyses describe the following:

1. A best estimate blind analysis of LOFT Test L3-6 was performed using the actual initial conditions and operational procedures of the test, but without using comparisons with the experimental data for modification of the blind analysis model.

2. A best estimate post-test analysis of LOFT Test L3-6 was performed utilizing information gained from analysis of the L3-6 data in order to identify changes to the blind analysis model which were required to improve the comparison between the analysis and data.

The results of the analyses presented in this report indicate that the methods used by C-E for small break analyses adequately predict small break experiments.

This report also contains a brief discussion of the impact of the post-test model changes on the analysis of a commerical PWR where the pumps are powered throughout the transient.

TABLE OF CONTENTS

Section	Title	Page
	LIST OF TABLES	v
	LIST OF FIGURES	vi
1.0	INTRODUCTION	1-1
	1.1 References for Section 1.0	1-2
2.0	LOFT FACILITY AND EXPERIMENT DESCRIPTION	2-1
	2.1 Description of LOFT Facility	2-1
	2.2 Description of the L3-6 Experiment	2-1
	2.3 References for Section 2.0	2-2
3.0	DISCUSSION OF L3-6 ANALYSIS	3-1
	3.1 Computer Program	3-1
	3.2 Pre-Test Model Setup	3-1
	3.3 Blind Analysis	3-2
	3.3.1 Calculational Model	3-2
	3.3.2 Blind Analysis Results	3-3
	3.3.3 Blind Analysis Conclusions	3-6
	3.4 Post-Test Analysis	3-6
	3.4.1 Goals	3-6
	3.4.2 Analytical Model Changes	3-7
	3.4.2.1 Best Estimate System Representation	3-7
	3.4.2.2 Improved Numerical and Physical Representation	3-8
	3.4.2.3 Break Flow Modeling	3-10
	3.4.3 Results	3-11
	3.4.3.1 Primary Coolant System (PCS) Pressure	3-11

TABLE OF CONTENTS, Continued

Section	Title	Page
	3.4.3.2 Secondary Side Pressure	3-11
	3.4.3.3 Primary Coolant System (PCS) Mass Balance	3-13
	3.4.4 Post-Test Analysis Conclusions	3-15
	3.5 References for Section 3.0	3-16
4.0	IMPACT ON PWR ANALYSIS	4-1
	4.1 Discharge Coefficient/Break Flow Model	4-1
	4.2 Piping to Coolant Heat Transfer	4-2
	4.3 Two-Phase Pump Head Degradation	4-2
	4.4 Non-Equilibrium Conditions in the Secondary Side	4-3
	4.5 Conclusions	4-4
	4.6 References for Section 4.0	4-4
5.0	CONCLUSIONS	5-1

LIST OF TABLES

Table	Title	Page
3-1	Description of CEFLASH-4AS Nodes	3-18
3-2	Description of CEFLASH-4AS Flowpaths	3-19
3-3	Differences Between the C-E Pre-Test Analysis of L3-6 and the Response to Bulletin 79-06C	3-21
3-4	L3-6 Post-Test Analysis. Predicted and Actual Integrated Break Flows.	3-22
3-5	L3-6 Post-Test Analysis. Predicted and Actual Mass Balances at Time of Pump Trip.	3-23

LIST OF FIGURES

Figure	Title	Page
3-1	LOFT L3-6 Pre-Test Model, Nodalization Diagram	3-24
3-2	LOFT L3-6 Blind Analysis, Nodalization Diagram	3-25
3-3	LOFT L3-6 Post-Test Analysis, Nodalization Diagram	3-26
3-4	LOFT L3-6 Blind Analysis, Primary System Pressure	3-27
3-5	LOFT L3-6 Blind Analysis, Break Flow	3-28
3-6	LOFT L3-6 Blind Analysis, Primary System Mass Inventory	3-29
3-7	LOFT L3-6 Blind Analysis, Pressure Drop Across Primary Coolant Pumps	3-30
3-8	LOFT L3-6 Blind Analysis, Secondary Side Pressure	3-31
3-9	LOFT L3-6 Blind Analysis, Inner Vessel Mixture Level	3-32
3-10	LOFT L3-6 Post-Test Analysis, Break Flow Quality Enhancement	3-33
3-11	LOFT L3-6 Post-Test Analysis, Primary System Pressure	3-34
3-12	LOFT L3-6 Post-Test Analysis, Inner Vessel Mixture Level	3-35
3-13	LOFT L3-6 Post-Test Analysis. Pressure Drop Across Primary Coolant Pumps	3-36
3-14	LOFT L3-6 post-Test Analysis, Secondary Side Pressure	3-37
3-15	LOFT L3-6 Steam Generator, Mixed Forward/Reverse Heat Transfer Mode	3-38
3-16	LOFT L3-6 Steam Generator Temperature Transients and Secondary Side Liquid Level Above Tube Sheet	3-39
3-17	LOFT L3-6 Post-Test Analysis, Break Flow	3-40
3-18	LOFT L3-6 Post-Test Analysis, Primary Coolant System Mass Inventory	3-41
4-1	LOFT L3-6 Primary System Pressure, Effect of Break Quality Enhancement	4-5
4-2	LOFT L3-6 Primary System Pressure, Effect of Break Discharge Coefficients	4-6

LIST OF FIGURES, Continued

Figure	Title	Page
4-3	LOFT L3-6 Primary System Energy Balance	4-7
4-4	C-E PWR, Primary System Energy Balance	4-8
4-5	Two Phase Head Degradation Coefficient	4-9
4-6	LOFT L3-6, Pressure Drop Across Primary Coolant Pumps. Effect of Two Phase Head Degradation Coefficient	4-10
4-7	LOFT L3-6, Primary System Pressure. Effect of Two-Phase Head Degradation Coefficient	4-11

1.0 INTRODUCTION

LOFT Test L3-6 was the sixth experiment in the LOFT Small Break Series and simulated a 0.1 ft^2 communicative break at the pump discharge of a commercial PWR. It differed from previous LOFT Small Break Tests in that the pumps remained powered throughout the test.

The United States Nuclear Regulatory Commission (NRC), in Reference 1-1, required that the C-E Owners' Group submit a "blind" analysis of LOFT Test L3-6. In order to obtain the necessary assurance that the analysis was a truly blind calculation, the NRC also required the submittal of the model to be used for the blind analysis prior to the running of the experiment. C-E met this pre-test requirement on December 1, 1980 with the submittal to the NRC of the L3-6 model (Reference 1-2).

LOFT Test L3-6 was run on December 10, 1980. The schedule, at that point, called for the release of the actual initial conditions and operational procedures by late January, 1981. The information was then to be reviewed by C-E and a schedule established for the submittal of the blind analysis (Reference 1-3).

On January 15, 1981, EG&G, Idaho briefed the NRC and the NSSS vendors on the results of LOFT Test L3-5 (pumps tripped) and L3-6 (pumps running). Since then, the L3-6 Quick Look Report (Reference 1-4) and the Experiment Data Report (Reference 1-5) were released. As was stated in Reference 1-3, C-E performed a review of the actual initial conditions and operational procedures and established an analysis submittal date of April 1, 1981 (Reference 1-6).

This report presents a blind analysis and a post-test analysis of LOFT Test L3-6. The analyses were performed by C-E for the C-E Owners' Group on Post TMI Efforts. The analyses describe the following:

1. A best estimate blind analysis of LOFT Test L3-6 which was performed using the actual initial conditions and operational procedures from the test (References 1-4, 1-5 and 1-7) but without using comparisons with the experimental data for modification of the blind analysis model (Section 3.3).

2. A best estimate post-test analysis of LOFT Test L3-6 which was performed utilizing information gained from analysis of the L3-6 data in order to identify changes to the blind analysis model which were required to improve the comparison between analysis and data (Section 3.4).

The report also contains a brief discussion of the impact of the post-test model changes on the analysis of a PWR where the pumps are powered throughout the small break LOCA transient.

1.1 REFERENCES FOR SECTION 1.0

1-1 Letter, P. S. Check, USNRC, to G. Liebler, C-E Owners' Group, Subject: Prediction Requirements for LOFT Small Break Test L3-6, Jur 26, 1980.

1-2 Letter, K. P. Baskin, C-E Owners' Group, to B. Sheron, USNRC, Subject: Calculational Model and Input for L3-6 Analysis, December 1, 1980.

1-3 Letter, G. Liebler, C-E Owners' Group, to P. S. Check, USNRC, Subject: Test Analysis of LOFT Small Break Test L3-6, July 15, 1980.

1-4 G. E. McCreery, "Quick-Look Report on LOFT Nuclear Experiment L3-6/ L8-1", EGG-LOFT-5318, December, 1980.

1-5 P. D. Bayless and J. M. Carpenter, "Experiment Data Report for LOFT Nuclear Small Break Experiment L3-6 and Severe Core Transient Experiment L8-1", NUREG/CR-1868, January, 1981.

1-6 Letter, K. P. Baskin, C-E Owners' Group, to P. S. Check, USNRC, Subject: Submittal Schedule for Analysis of LOFT Test L3-6, February 13, 1981.

1-7 Letter, L. P. Leach, Manager LOFT Department, to R. E. Tiller, DOE, Subject: Post-Test Information for L3-6 Required Problem", LPL-175-81, January 7, 1981.

2.0 LOFT FACILITY AND EXPERIMENT DESCRIPTION

2.1 DESCRIPTION OF LOFT FACILITY

The LOFT facility for Test L3-6 consists of a reactor vessel, an operating loop, and an inactive loop. The operating loop consists of an active steam generator, a pump U-bend, and two primary coolant pumps operating in parallel. The inactive loop contains a hot leg and a cold leg which had been connected to a blowdown suppression tank during previous LOCA experiments. For the L3-6 test the break was placed at the pump discharge of the operating loop. The break orifice was located at the end of a pipeline connected to the side of the intact loop cold leg at its centerline. The inactive hot and cold legs were isolated from the blowdown suppression tank. A core bypass flowpath existed due to leaking isolation valves in the reflood assist bypass system. Further details of the LOFT facility are available in References 2-1 through 2-5.

2.2 DESCRIPTION OF THE L3-6 EXPERIMENT

LOFT Test L3-6 was run on December 10, 1980 at Idaho National Engineering Laboratory. The test simulated a 0.1 ft^2 communicative break at the pump discharge of a large PWR. The primary difference between LOFT Test L3-6 and previous small break tests at the LOFT facility was that the primary coolant pumps remained powered at a constant speed throughout the transient.

The L3-6 transient was initiated by scramming the reactor which was at full power (50 Mwt). Upon receipt of a signal that the control rods were fully inserted, the break was opened. Only emergency core coolant injection with the high pressure pumps was available for the experiment. The experiment continued until the primary side pressure decreased to ~350 psia. At that point the primary coolant pumps were tripped ending the L3-6 experiment. Further details of the experiment are presented in References 2-7 and 2-8 and in Section 4.0 of this report.

2.3 REFERENCES FOR SECTION 2.0

2-1 D. L. Reeder, "LOFT System and Test Description (5.5 ft Nuclear Core 1 LOCES)", TREE-1208, July, 1978.

2-2 Letter, N. C. Kaufman (EG&G, ID.) to R. E. Tiller (DOE, ID.), Subject: L3-6 Information Package, Kau-29-80, February 5, 1980.

2-3 Letter, N. C. Kaufman (EG&G, ID.) to R. E. Tiller (DOE, ID.), Subject: Revision to L3-6 Information Package, Kau-34-80, February 15, 1980.

2-4 Letter, N. C. Kaufman (EG&G, ID.) to R. E. Tiller (DOE, ID.), Subject: Revised L3-6 Required Problem Information Package, Kau-181-80, August 18, 980.

2-5 Letter, N. C. Kaufman (EG&G, ID.) to R. E. Tiller (DOE, ID.), Subject: L3-6 Required Problem Additional Information, Kau-222-80, September 17, 1980.

2-6 Letter, L. P. Leach (EG&G, ID.) to R. E. Tiller (DOE, ID.), Subject: Post-Test Information for L3-6 Required Problem, LPL-175-81, January 7, 1981.

2-7 P. D. Bayless, J. M. Carpenter, "Experiment Data Report for LOFT Nuclear Small Break Experiment L3-6 and Severe Core Transient Experiment L8-1", NUREG/CR-1868, January, 1981.

2-8 G. E. McCreery, "Quick Look Report on LOFT Nuclear Experiment L3-6/L8-1", EGG-LOFT-5318, December, 1980.

3.0 DISCUSSION OF L3-6 ANALYSIS

The analysis of L3-6 is divided into three phases: pre-test setup of the model, a "blind" analysis and a post-test analysis. This section will discuss the generation of the model and the results of the analysis with comparisons to test data where applicable.

3.1 COMPUTER PROGRAM

The hydraulic analysis of L3-6 was performed using a modified version of the CEFLASH-4AS code documented in Reference 3-1. The modifications were incorporated as a result of a continuing development of a best estimate small break model. The modified version was used in the following analyses:

a) CEN-114 (Reference 3-2)
b) CEN-115 (Reference 3-3)
c) Analysis of LOFT Test L3-1 (Reference 3-4)
d) Analysis of Semiscale MOD-3 Test S-07-10B (Reference 3-5)

In addition to model changes, improvements have been made to the code in order to reduce the execution time. These improvements, however, did not affect the calculated results.

3.2 PRE-TEST MODEL SETUP

The nodalization of the LOFT facility for Test L3-6 is based on the nodalization used for the C-E analysis of Test L3-1 (Reference 3-4). The L3-1 nodalization (i.e. control volumes, flowpaths) was modified to reflect hardware changes in the system between L3-1 and L3-6. A nodal diagram for the pre-test model is shown in Figure 3-1. A description of the nodes and flowpaths shown in Figure 3-1 is given in Tables 3-1 and 3-2, respectively. The modelling rationale (i.e. flow regime within the control volume, etc.) was governed by the model used in CEN-115 (Reference 3-3). The pre-test model for L3-6 differed from the pumps-running model presented in CEN-115 by the component models shown in Table 3-3. Table 3-3 shows that only those models required to do a best

estimate calculation of L3-6 were changed. This model was submitted to the NRC on December 1, 1980 (Reference 3-6) as required by the NRC.

3.3 BLIND ANALYSIS

3.3.1 Calculational Model

LOFT Test L3-6 was run on December 10, 1980. The actual initial conditions and operational procedures were received in late January, 1981 (Reference 3-7). Upon review of the actual initial conditions and procedures, the model was changed to reflect the actual test in the following areas:

1. Pump Speed

   In the pre-test model, the pumps were allowed to overspeed due to lack of hydraulic torque degradation when pumping two-phase. In L3-6 the pump speed was held constant at approximately the steady state speed. The pump model was modified to maintain a constant speed during the transient.

2. Primary Coolant Pump Injection

   The pre-test model did not include the primary coolant pump injection. The primary coolant pump injection was included in the blind analysis for completeness. Figure 3-2 reflects this addition.

3. Main Steam Valve Cycling

   The main steam valve was observed to have been cycled open and closed ~85 seconds after the break opened. This was included in the blind analysis.

4. Miscellaneous Timing of Events

   The operator controlled events differed slightly from those specified by the pre-test information supplied by EG&G.

These included break opening time relative to scram, HPSI initiation pressure, time of auxiliary feedwater initiation and termination, and main steam valve closure time. The timing of these events was properly represented in the blind analysis.

5. Initial Pressures/Conditions

The conditions in the primary system (power, flow, pressure) for the test were acceptably close to the pre-test values specified by EG&G. Therefore, they were not changed for the blind analysis. The actual secondary pressure, however, was higher than anticipated (807 psia vs. 757 psia), and was adjusted accordingly.

The changes summarized above were made without use of the experimental results. The analysis presented in Section 3.3.2 is, therefore, a blind analysis.

3.3.2 Blind Analysis Results

The analysis discussed in this section is a blind analysis of LOFT Test L3-6. It was performed using the actual initial conditions and operational procedures as summarized in Section 3.3.1. Although the experimental results were available at the time of the blind analysis, they were not used in the selection of the blind analysis models. The experimental data from L3-6 is presented along with the analysis results for completeness.

Figure 3-4 shows the primary system pressure compared to the experimental data from Test L3-6. It shows reasonable agreement between data and the analysis up to ~800 seconds after which the analysis depressurizes much faster than the data. This diversion at 800 seconds is caused by the wall heat in the downcomer. The wall heat i the LOFT facility is a dominant heat source and will be discussed in the post-section of this report (Section 3.4) and in Section 4 which discusses the impact of LOFT on the analysis of commercial PWR's.

There is a second break in the pressure at ~1100 seconds. The break is due to a transition from two-phase to steam at the break. Although the break in the experiment did ultimately go to a high quality flow, the transition occurred much later and was less abrupt. The reasons for the differences between the data and the analysis in the later half of the transient is due primarily to the use of the HEM critical flow correlation with a discharge coefficient of unity. That is, the break flow rate (Figure 3-5) was higher than the data in the initial portion of two-phase flow out of the break. Therefore, the break went to a steam flow condition earlier than the data. The post-test section of this report discusses modeling of the break for L3-6.

Another parameter of interest is the transient mass inventory of the primary system. Figure 3-6 compares the primary system mass inventory calculated by the CEFLASH-4AS code to the mass inventory from the test as calculated by EG&G. Although the final CEFLASH-4AS inventory is higher than the EG&G calculated inventory, there is reason to believe that the EG&G calculated final inventory is lower than the actual test results. The reasons for this statement are as follows.

A mass balance of the system is defined by Equation 3-1.

$$\text{INITIAL MASS INVENTORY} + \int_t (\text{HPSI FLOW})\,dt + \int_t (\text{PCP INJECTION})\,dt - \int_t (\text{BREAK FLOW})\,dt = \text{MASS REMAINING} \qquad (3\text{-}1)$$

During the initial 800 seconds of the transient, the calculated system pressure is essentially the same as the data (Figure 3-4). This means that HPSI pump flow is the same as the data since the HPSI pump flow is a function of pressure. The PCP injection flowrate is controlled by positive displacement pumps and is, therefore, a constant. This leaves the integrated break flowrate as the controlling factor in the system mass balance for the first 800 seconds of the transient. As was pointed out earlier, the C-E blind analysis overpredicted the break flowrate measured by EG&G during the first 800 seconds of the transient. Since the break flowrate was used by EG&G (Reference 3-11) for the calculation of the system inventory, and the

C-E calculation overpredicts the break flow for the first 800 seconds, the C-E calculated mass inventory should be significantly lower than the EG&G calculation. It, however, matches the EG&G calculation reasonably well.

This implies that either the mass inventory reported by EG&G is lower than the actual value or that the actual mass flow was higher than the reported data. In either case the data is inconsistent and therefore subject to question. A further discussion of the mass inventory is presented in Section 3.4.3.3.

Figure 3-7 shows the comparison between the blind calculated and measured pump head. The analysis shows that the pump head degrades more quickly than the data. This was due to the two-phase head degradation model used in the blind analysis. The degradation model was the same as the one used in CEN-115 and is based on pump tests performed by the Aerojet Nuclear Corporation. This model degrades the pump head at relatively low void fraction (~15%). Although this comparison might be improved through the use of a different two-phase head degradation model, little effect on the system behavior is expected. This aspect is further discussed in Section 4.0 of this report.

The secondary side pressure comparison is shown in Figure 3-8. There is good agreement with the data up to approximately 900 seconds, when the calculated pressure falls below the data. This deviation is linked to the thermal equilibrium assumption used for the secondary side model, and will be discussed in Section 3.4.3 of this report.

The final comparison is for the two-phase mixture level in the reactor vessel. Figure 3-9 shows that at ~1300 seconds the mixture level is calculated to fall below the top of the core. This results in a few degrees superheat

on the cladding surface. Although the data does not explicitly show a mixture level in the core, EG&G has calculated that the uninstrumented rods in the core experienced 36°F to 144°F of superheat prior to pump trip (Reference 3-8). This is qualitatively consistent with the C-E blind analysis result.

3.3.3 Blind Analysis Conclusions

The blind analysis presented in Section 3.3.2 qualitatively predicted the data. Although the timing and magnitude of specific parameters were somewhat off, the analysis in general predicted the system behavior of a LOFT small break with the pumps running.

3.4 POST-TEST ANALYSIS

The open phase of the post-test analysis of LOFT Test L3-6 was carried out in order to define modelling changes which would provide a more accurate prediction of the L3-6 experiment, beyond the degree achieved in the blind analysis. The goals of the post-test analysis and its results are described below.

3.4.1 Goals

The open post-test analysis was carried out with a three-pronged goal. The first goal was to create a best-estimate prediction model which reflects as closely as possible those LOFT system parameters and actual test conditions which are peculiar to the LOFT facility and were not included in the blind analysis.

The second goal was to resolve several instances of localized non-physical behavior which were observed in the blind phase of the analysis described in Section 3.3 of this report. All but one of these anomalies were directly related to unique aspects of the LOFT system.

The third goal of this analysis was to address the ever-present uncertainty in the calculation of break flow rate.

3.4.2 Analytical Model Changes

The analytical model used in the post-test analysis was based on the one used in the blind analysis. That is, it included all of the modelling changes which were described in Section 3.3.1. The modelling changes required to accomplish the goals of the post-test analysis are as follows:

3.4.2.1 Best Estimate System Representation

The first goal of accurately modeling the LOFT facility and actual test conditions in a best-estimate analysis required the following model changes relative to the blind analysis.

- The effect of wall heat was introduced into the steam generator secondary side node. Wall heat is a modeling of the thermal interaction which takes place between the coolant fluid and the system's internal metal structures. Most of the primary system nodes contained a wall heat model, as indicated by heat slabs in Figure 3-3.

- A leak in the steam generator steam valve was added in order to account for the steam valve leak reported in Reference 3-7.

- The initial mass inventory in the steam generator secondary side was increased by 35%, to agree with the actual initial conditions.

- The rate of heat generated by the primary coolant pumps and added to the fluid was made proportional to the rate of mass being pumped. Pump heat in the blind analysis had been modeled with a constant rate. The change to a variable pump heat rate was in accordance with Reference 3-9. It resulted in a reduction of 86% in the total heat added to the primary coolant by the pumps during the transient, or to ~4% of the total core decay heat.

- The primary coolant pump injection (PCPI) flow, which in the blind analysis had been directed into the pump discharge cold leg

(Figure 3-2), was split and re-directed into the two loop seal risers (Figure 3-3). This permitted the pumps to "see" the PCPI liquid, more closely approximating the actual direct injection into the pump housing.

- Reverse heat transfer in the steam generator's primary side was re-modeled with the Dittus-Boelter correlation for convective heat transfer to steam. This replaced the artificially high reverse heat transfer coefficient which the blind analysis model had adopted from the CEN-115 version of CEFLASH-4AS, bringing the post-test analysis model closer to a best-estimate model.

3.4.2.2 Improved Numerical and Physical Representations

The following model modifications were implemented as part of the second goal of the post-test analysis, having been necessitated by several instances of localized anomalous behavior which were observed in the blind analysis results. These observations and the corresponding model changes are described below.

- The two downcomer nodes, which in the blind analysis had been handled with a mixed homogeneous/heterogeneous algorithm, were re-modeled as homogeneous-mixture nodes. This change was made in response to an observation in the blind analysis that the heterogeneous mixture in the upper half downcomer node was draining into the lower half downcomer node in a non-physical manner.

- The wall heat representation in homogeneous-mixture nodes was revised. Wall heat, the thermal interaction between coolant and internal metal structures, had been modeled in the blind analysis as proportional to the mixture level in each individual node. Homogeneous-mixture nodes, however, were treated as being always full as long as the mixture quality was less than unity, resulting in overpredicted wall heat rates. For PWR's, the error is negligible, shortening the time in which the metal structures reach thermal equilibrium with the fluid, as they all inevitably must. Thus, the total amount of energy transferred to the fluid is unaffected.

While this generality has always been true for all full-scale PWRs (see Section 4.0) and for most components of the LOFT facility, the LOFT downcomer presented a unique, notable exception. The abnormally massive walls of the LOFT downcomer acted as a nearly infinite heat source and did not approach thermal equilibrium with the primary coolant within the transient time of the LOCE. Thus, the homogeneous-mixture downcomer model erroneously introduced a tremendous amount of additional wall heat into the system, a modeling aberration unique to the LOFT facility.

A simple modeling change was therefore implemented for all homogeneous-mixture nodes, in which the wall heat rate was made proportional to the theoretical, fully-collapsed liquid level of the mixture. While this in itself tended to underpredict the wall heat, it apparently created a fairly reasonable description of wall-fluid thermal interactions when combined with the conduction-limited (infinite convective heat transfer coefficient) wall heat transfer model of CEFLASH-4AS.

- The node representing the hot leg side of the leaking reflood assist bypass line was homogenized due to its observed non-physical draining behavior in the blind analysis. This behavior was similar to that which had been observed in the downcomer. Although the pipe in question, a part of the inactive loop, certainly did not contain a homogeneous mixture, the change had a negligible effect on the overall transient. This situation is unique to the LOFT system with its bypass leak in an inactive loop.

- The flow path connecting the downcomer node to the inactive loop cold leg node (Figure 3-2, path 14) was split into two parallel paths (Figure 3-3, paths 14 and 25) between the same two nodes. This change was implemented in order to properly model the flow between the downcomer and the inactive cold leg -- another LOFT peculiarity.

3.4.2.3 Break Flow Modeling

The third goal of the post-test analysis was to address the uncertainty which traditionally accompanies the calculation of the break flow rate. This break flow uncertainty was demonstrated in the C-E analysis of LOFT Test L3-1 (Reference 3-4). In the post-test analysis, the question was resolved by analyzing the break flow data of the L3-6 Test (Reference 3-10) and deriving from it those break parameters which relate to the characteristics of the particular break orifice and the particular break geometry of LOFT Test L3-6. The following conclusions were reached and corresponding model changes implemented.

- The effective break area was decreased by 15%. This change was based on test data for the break flow rate and on the pressure and density measurements in the break spool piece upstream of the orifice. Comparison of the actual break flow to that predicted by the homogeneous equilibrium model (HEM) for critical flow showed an equivalent break area which varied from 83% of the actual area of the break orifice for saturated water to 100% for saturated steam. Since most of the mass loss occurred during the subcooled-liquid and low-quality mixture portions of the transient, a break area multiplier of 0.85 was chosen.

- A break flow quality enhancement model was implemented in the CEFLASH-4AS code. It was based on a phenomenon, demonstrated by the test data in which the quality of the two-phase mixture in the break piping upstream of the orifice exceeded that of the two-phase mixture in the cold leg just upstream of the break piping. This quality-enhancement phenomenon was due to the unequal inertial forces acting on the steam and on the small, intermediate and large sized water droplets in the mixture, as the mixture executed the required 90° turn in order to enter the break pipe. The functional relationship between break flow quality and cold leg quality is probably strongly dependent on the break geometry -- i.e., the diameter of the break pipe where it joints the cold leg, as well as the break orientation (bottom, middle or top of cold leg). Since the blind analysis used the same quality for the break flow

and the cold leg, a quality enhancement function was derived from the data and was implemented for the post-test analysis. Use of this quality enhancement function provided for a higher quality for the break flow relative to that of the cold leg, as shown in Figure 3-10.

3.4.3 Results

3.4.3.1 Primary Coolant System (PCS) Pressure

The post-test analysis is C-E's best-estimate test prediction using conditions and methodologies which best reflect the actual running conditions of the test. Figure 3-11 compares the predicted and measured (Reference 3-10) primary coolant system pressures. The agreement of analysis with data is excellent during most of the transient. The underprediction of pressure, which showed up at 1400 seconds, peaked at 90 psi at 1600 seconds, and gradually vanished thereafter.

The discontinuity which can be seen in the rate of predicted PCS depressurization at 1460 seconds was due to voiding of the active loop. At that time, the level of the two-phase mixture in the reactor vessel, which had been slowly sinking at a rate of 0.28 in/min for approximately 20 minutes, finally fell below the bottom lip of the reactor vessel outlet nozzle, as shown in Figure 3-12. With two-phase no longer feeding the steam generator, the entire primary side of the steam generator and the loop seals voided of all liquid and sent steam into the PCS pumps. The resulting sudden loss of pump head (Figure 3-13) caused the abrupt drop of the reactor vessel mixture level seen in Figure 3-12.

3.4.3.2 Secondary Side Pressure

Figure 3-14 compares the predicted and measured pressures in the secondary system. The agreement of analysis with data is excellent during the first 1000 seconds. Thereafter, the system is in a reverse heat transfer mode (on the basis of pressure), and the predicted and measured secondary side pressures differ.

The underlying cause of this widening discrepancy lies in the one-node thermal equilibrium treatment of the steam generator secondary side by the CEFLASH-4AS code. Figure 3-15 shows a schematic of actual conditions in the steam generator in a reverse heat transfer mode. Cold auxiliary feedwater collects at the bottom of the steam generator, forming a subcooled layer (A). A region of hot water (B) sits atop the subcooled layer, with steam in the dome (C). Thus, with forward heat transfer taking place in the subcooled layer and reverse heat transfer in the saturated layer, the net heat exchange with the primary fluid is greatly reduced. Except for a small leak, the main steam valve is closed during the test. With mass and energy transfers out of the steam generator secondary side drastically reduced, auxiliary feedwater continues to collect in the subcooled layer, raising the liquid level, thus supporting the pressure in the trapped steam in the steam generator dome.

This scenario of the actual conditions which existed in the steam generator during LOFT Test L3-6 are clearly corroborated by data (Reference 3-10). Figure 3-16 shows the steam generator's measured temperature transients. The primary fluid temperatures were measured in the inlet and outlet plena, the subcooled water temperature was measured at the bottom of the downcomer and therefore represents the water temperature just above the tube sheet. The saturation temperature is based on the measured pressure in the steam generator dome. As the figure clearly indicates, the liquid region was kept well homogenized during the first 400 seconds of strong forward heat transfer by free convection and the formation of steam bubbles. Temperature stratification began at 400 seconds and grew more pronounced throughout the transient. A period of simultaneous forward and reverse heat transfer began at 1150 sec and persisted throughout the transient. The liquid level in the steam generator secondary is also shown in Figure 3-16 and confirms our previous discussion. The level stopped increasing at 1856 seconds when the auxiliary feedwater was shut off, resulting in a decidedly faster rate of secondary system depressurization (see Figure 3-14).

The CEFLASH-4AS steam generator model is unable to handle the non-equilibrium conditions described above. The code models the steam generator secondary side node as a two-region (liquid and steam), one-temperature (saturated)

system. Subcooled auxiliary feedwater is, in effect, instantaneously and uniformly mixed with the saturated liquid inventory, necessitating a simultaneous condensation of steam in order to maintain saturation conditions. Thus, the auxiliary feedwater in an equilibrium representation has a depressurizing effect on the secondary side. As can be seen in Figure 3-14, the shutoff of auxiliary feedwater at 1856 seconds resulted in a decidedly slower calculated rate of secondary system depressurization. The effect of the existing steam generator equilibrium model on primary coolant system behavior was minimal, as was observed in Figure 3-11. Section 4.0 further discusses this aspect of the post-test analysis.

3.4.3.3 Primary Coolant System (PCS) Mass Balance

LOFT Test L3-6 demonstrated the maintenance of adequate core cooling during a loss of coolant event in which the pumps were powered, even when a major portion of the primary fluid had been lost. After the primary coolant pumps are finally tripped, however, the ability of the system to provide the core with adequate cooling depends, in part, on the primary coolant mass inventory remaining in the system at the time of pump trip.

The L3-6 post-test analysis predicted a final mass inventory at the end of Test L3-6 (2371 sec) of 3138 lbm. This appears to be quite high when compared with the final inventory of 1496 lbm which was reported by EG&G (Reference 3-12).

In order to trace the causes of this difference, the PCS mass balance was examined in detail. In the L3-6 experiment, mass entered and exited the PCS at three points -- high pressure injection (HPSI), primary coolant pump injection (PCPI) and break flow. Of these, the HPSI and PCPI flows were predicted correctly, since the former was a function of pressure which was predicted accurately (Figure 3-11), and the latter was delivered at a constant rate by a positive displacement pump. Thus, only the break flow need be considered for a mass inventory comparison.

The break flow during LOFT Test L3-6 exhibited two distinct regimes -- subcooled break flow during the first ~50 seconds and two-phase thereafter. (Because of the PCPI, the break flow never went to pure steam). Since break flow measurements were not available for the first 50 seconds of the test, the subcooled break flow was reconstructed by using the Henry-Fauske critical flow correlation with a discharge coefficient of 0.97. Measured pressures and temperatures (Reference 3-10) in the break piping upstream of the orifice were used in evaluating the critical flow. The choice of correlation and discharge coefficient was based on Reference 3-11. The result of this calculation is presented in Table 3-4, and was corroborated by a similar calculation performed by EG&G (Reference 3-11). As the table shows, the post-test analysis, which used the homogeneous equilibrium model for critical flow with a discharge coefficient of 0.85, underpredicted the subcooled break flow.

During the period following transition to two-phase flow, the post-test analysis matched very well with the measured break flow data, as shown in Figure 3-17. Indeed, table 3-4 shows that the post-test analysis underpredicted total break flow by only 5.2% during that period.

Thus, for the overall transient, the sum of the post-test analysis underpredictions of break flow appears to account for only half of the difference in mass inventory reported above.

The key to this inconsistency lies within the measured and calculated data reported by EG&G. Table 3-5 summarizes the mass balances of the post-test analysis prediction and the actual experiment. The table shows the actual final inventory, as calculated from the published data, both by C-E and by EG&G (Reference 3-11), to be 2203 lbm, and the post-test analysis overprediction to be considerably less severe than reported above. Figure 3-1 shows the transient of the actual mass inventory, as well as the post-test analysis prediction.

There appears to be, then, an internal inconsistency between the L3-6 final mass inventory calculated by C-E and EG&G from the data in Reference 3-10 (2203 lbm) and the mass inventory reported by EG&G in Reference 3-12 (1496 lbm). At present, this difference has not been resolved.

Additional calculations were made to determine the possible effect on the system's final mass inventory if further model changes were made to improve the match between calculated pressure and experimental data beyond about 1200 seconds. This would prevent total uncovery of the reactor vessel outlet nozzle and voiding of the active loop, which would increase the break flow. These calculations showed that the resultant improvements in break and HPSI flows would decrease the final inventory to ~2050 lbm. This encouraging result appears to account for the difference between the actual final mass inventory and the one calculated by CEFLASH-4AS.

3.4.4 Post-Test Analysis Conclusions

The post-test analysis presented in Section 3.4 was performed using information obtained from analysis of the L3-6 data in order to identify parameters of the LOFT system behavior when the pumps are running. The post-test analysis did an outstanding job of predicting the primary coolant system pressure and the break flow. The secondary side pressure prediction was excellent during the period of forward (primary to secondary) heat transfer in the steam generator, but deteriorated rapidly during reverse heat transfer, with negligible effect on the primary system. The PCS mass inventory was overpredicted, but the difference could not be precisely quantified because of an internal inconsistency in the data.

3.5 REFERENCES FOR SECTION 3.0

3-1 CENPD-133, Suoplement 1, "CEFLASH-4AS, A Computer Program for the Reactor Blowdown Analysis of the Small Break Loss-of-Coolant Accident", August, 1974.

CENPD-133, Supplement 3, "CEFLASH-4AS, A Computer Program for the Reactor Blowdown Analysis of the Small Break Loss of Coolant Accident", January, 1977.

3-2 CEN-114-P, Amendment 1-P, "Review of Small Break Transients in C-E Nuclear Steam Supply Systems", July, 1979.

3-3 CEN-115-P, "Response to NRC IE Bulletin 79-06C, Items 2 and 3 for C-E Nuclear Steam Supply Systems", August, 1979.

3-4 "Combustion Engineering Analysis of LOFT Test L3-1", February, 1980.

3-5 Letter, George Liebler (C-E Owners' Group) to Dr. Denwood F. Ross (NRC), Subject: Semiscale S-07-10B Small Break Test, November 30, 1979.

3-6 Letter, K. P. Baskin (C-E Owners' Group) to Dr. Brian Sheron (NRC), Subject: Calculational Model and Input for L3-6 Analysis, December 1, 1980.

3-7 Letter, L. P. Leach (EG&G) to R. E. Tiller (DOE, ID), Subject: Post-Test Information for L3-6 Required Problem, LPL-175-81, January 7, 1981.

3-8 R. A. Nelson, "Fuel Rod Clad Temperature Measurements in L3-6", presentation given to NRC, January 15, 1981.

3-9 D. L. Reeder, "LOFT System and Test Description (5.5 ft Nuclear Core 1 LOCES)", TREE-1208, July, 1978.

3-10 P. D. Bayless and J. M. Carpenter, "Experiment Data Report for LOFT Nuclear Small Break Experiment L3-6 and Severe Core Transient Experiment L8-1", NUREG/CR-1868, January, 1981.

3-11 Private communication, D. L. Batt (EG&G) to S. Leichtberg (C-E), March 16-17, 1981.

3-12 J. H. Linebarger, "L3-6/L8-1 Results and L3-5/L3-6 Data Comparisons", handouts to NRC, January 15, 1981.

Table 3-1

Description of CEFLASH-4AS Nodes

Node	Description
1	Core, upper and lower plenums
2	Pressurizer and pressurizer surge line
3	Intact loop hot leg including outlet nozzle, steam generator inlet plenum and inlet tube sheet
4	½ of steam generator tubes
5	½ of steam generator tubes
6	Outlet tube sheet, outlet plenum, pump suction piping to ILPS #15
7	½ of ILPS #15, ½ of pump #1
8	½ of ILPS #15, ½ of pump #2
9	½ pump #1, ½ pump #2, intact loop cold leg discharge piping, reactor vessel inlet nozzle
10	Downcomer region, core bypass region
11	Upper downcomer region
12	Condenser at discharge of main steam line
13	Reactor vessel outlet nozzle to BLPS #4
14	BLPSs 49 through 56
15	½ of steam generator simulator
16	½ of steam generator simulator plus pump simulator
17	Piping assembly from pump simulator to isolation valve
18	BLPSs 40 through 46
19	Broken cold leg piping assembly plus reactor vessel inlet nozzle
20	Suppression tank
21	Steam generator secondary

ILPS - Intact loop piping section

BLPS - Broken loop piping section

Table 3-2

Description of CEFLASH-4AS Flowpaths

Flowpath	Description
1	Downcomer to inner vessel lower plenum
2	One half of piping from inner vessel upper plenum to intact loop hot leg node
3	One half of piping from inner vessel upper plenum to intact loop hot leg node
4	Pressurizer to intact loop hot leg node
5	One half of piping from intact loop hot leg node to hot side steam generator node
6	One half of piping from intact loop hot leg node to hot side steam generator node
7	Hot side steam generator node to cold side steam generator node
8	Cold side steam generator node to steam generator outlet plenum/ loop seal node
9	Steam generator outlet plenum/loop seal node to pump #1 loop seal node
10	Steam generator outlet plenum/loop seal node to pump #2 loop seal node
11	Pump #1 loop seal node to intact loop cold leg node
12	Pump #2 loop seal node to intact loop cold leg node
13	Intact loop cold leg node to downcomer node
14	Downcomer node to broken loop cold leg node
15	Reflood assist bypass system to broken loop cold leg node
16	One half of piping from inner vessel upper plenum to broken loop hot leg node
17	One half of piping from inner vessel upper plenum to broken loop hot leg node
18	Reflood assist bypass section to broken loop hot leg node
19	One half of piping from broken loop hot leg node to broken loop steam generator simulator

Table 3-2 (Cont'd)

Description of CEFLASH-4AS Flowpaths

Flowpath	Description
20	One half of piping from broken loop hot leg node to broken loop steam generator simulator
21	Connection between two vertical sections of steam generator simulator
22	Connection between pump simulator and node representing the piping between the pump simulator and the isolation valve
23	RABS path
24	Upper downcomer to lower downcomer
25	Broken cold leg to downcomer (post-test only)
26	PCP injection (blind and post-test only)
27	High pressure injection pump
28	Auxiliary feedwater
29	Leak flow path
30	PCP injection (post-test only)

Table 3-3

Differences Between the C-E Pre-Test Analysis of L3-6 and the Response to Bulletin 79-06C

Model	Bulletin 79-06C Analysis	L3-6 Analysis
Decay Heat	1.0 ANS Standard	LOFT Decay Heat
Power History	100% infinite operation	100% 40 hours operation
Break Flow Correlation	0.7 Moody	1.0 HEM
ECCS Availability	LPSI, HPSI, SIT	HPSI

Table 3-4

L3-6 Post-Te Analysis

Predicted and Actual Integrated Break Flows

(in lbm and % of initial mass inventory)

Time Period	Post-Test Analysis		Actual Test*		Difference Analysis-Test	
	lbm	%	lbm	%	lbm	%
0-50 sec	1,043	8.5	1,351	11	-308	-2.5
50-2371 sec	11,142	91.5	11,747	96.5	-605	-5
0-2371 sec	12,185	100	13,098	107.5	-913	-7.5

* From critical flow correlation during 0-50 sec, and LOFT Test L3-6 break flow data during 50-2371 sec.

Table 3-5

L3-6 Post-Test Analysis

Predicted and Actual Mass Balances at Time of Pump Trip

(in lbm and % of initial mass inventory)

	Post-Test Analysis		Calculated From Data		Reported by EG&G	
	lbm	%	lbm	%	lbm	%
Initial Inventory	12,200	100	12,161	100	12,161	100
Total HPSI	2,613	22	2,630	22(1)	2,630	22
Total PCPI	510	4	510	4(2)	510	4
Total Break	12,185	100	13,098	108(3)		
Final Inventory	3,138	26	2,203	18	1,496	12

(1) Integrated measured flow rate.

(2) 2371 sec. times constant flow rate.

(3) Table 3-4.

FIGURE 3-1

LOFT L3-6 PRE-TEST MODEL
NODALIZATION DIAGRAM

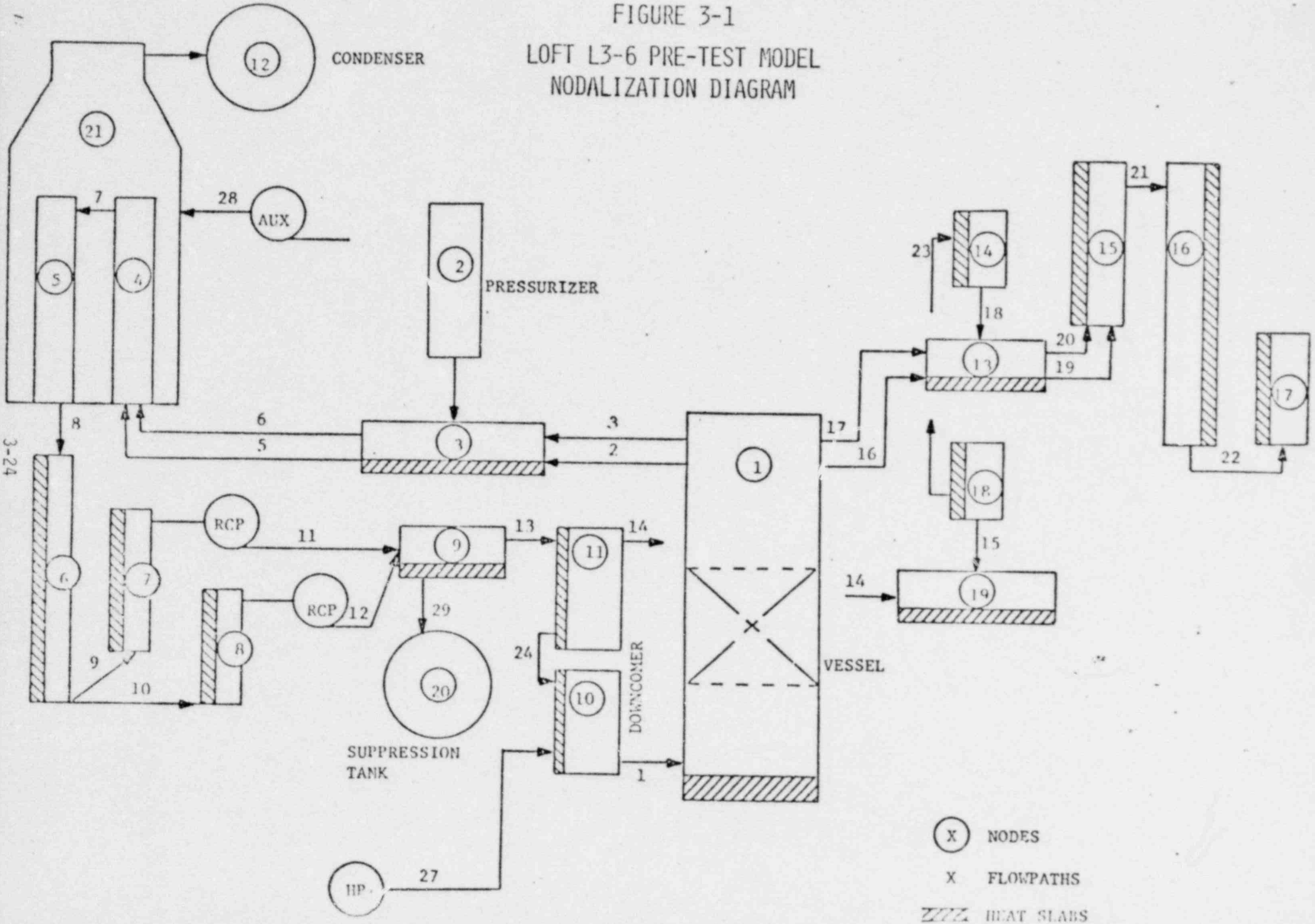

FIGURE 3-2

LOFT L3-6 BLIND ANALYSIS
NODALIZATION DIAGRAM

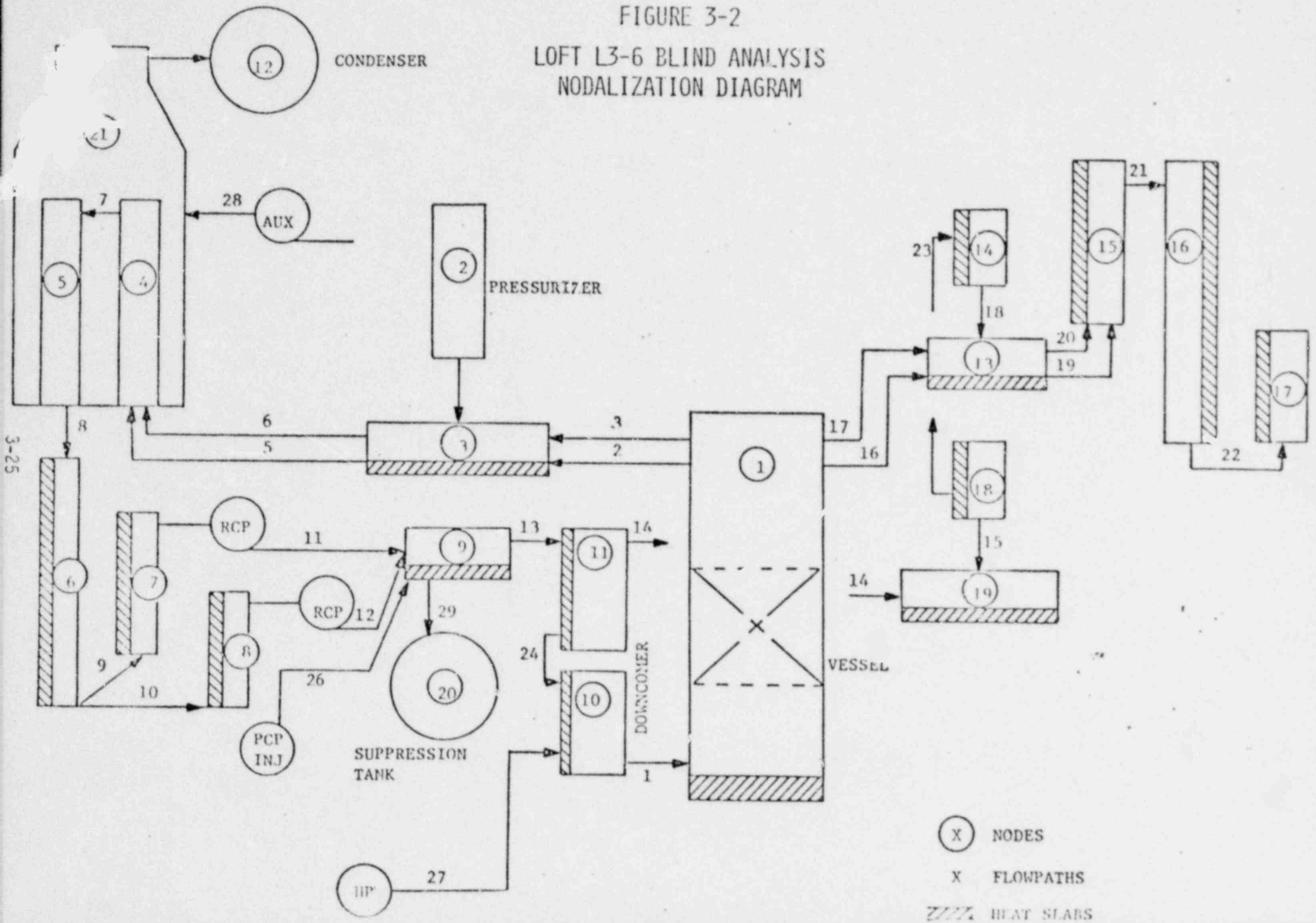

FIGURE 3-3

LOFT L3-6 POST-TEST ANALYSIS
NODALIZATION DIAGRAM

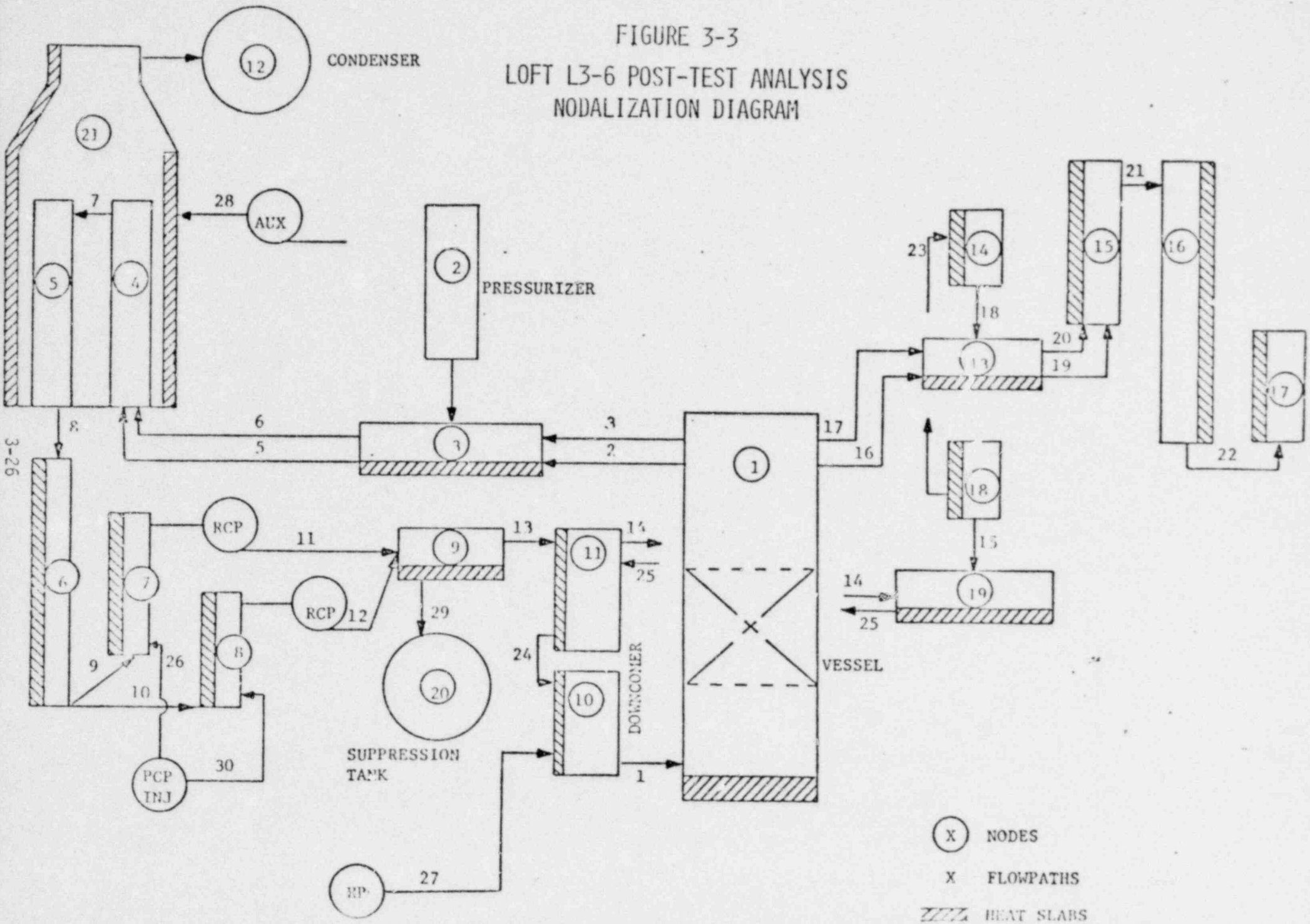

FIGURE 3-4

LOFT L3-6 BLIND ANALYSIS
PRIMARY SYSTEM PRESSURE

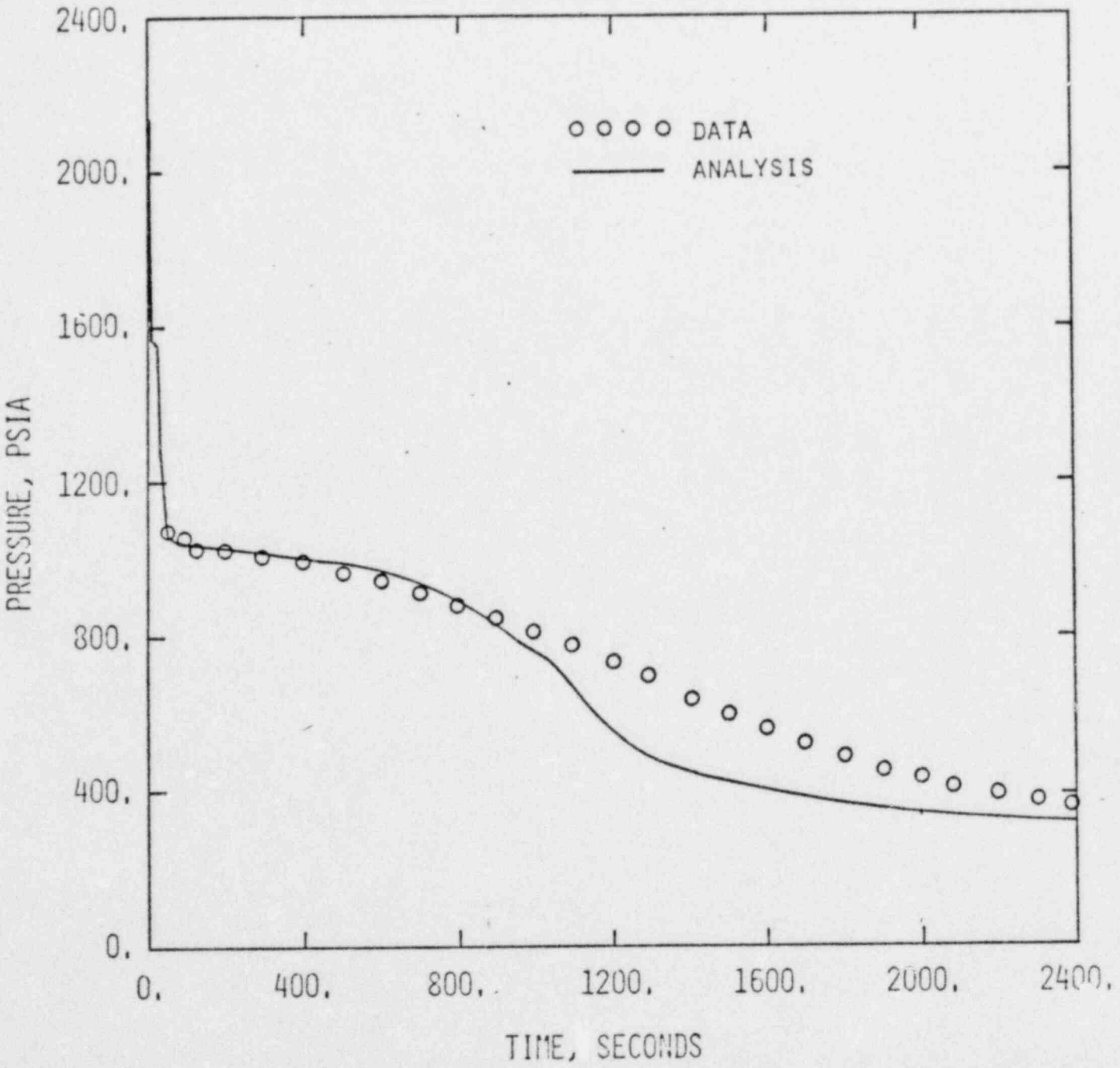

FIGURE 3-5

LOFT L3-6 BLIND ANALYSIS
BREAK FLOW

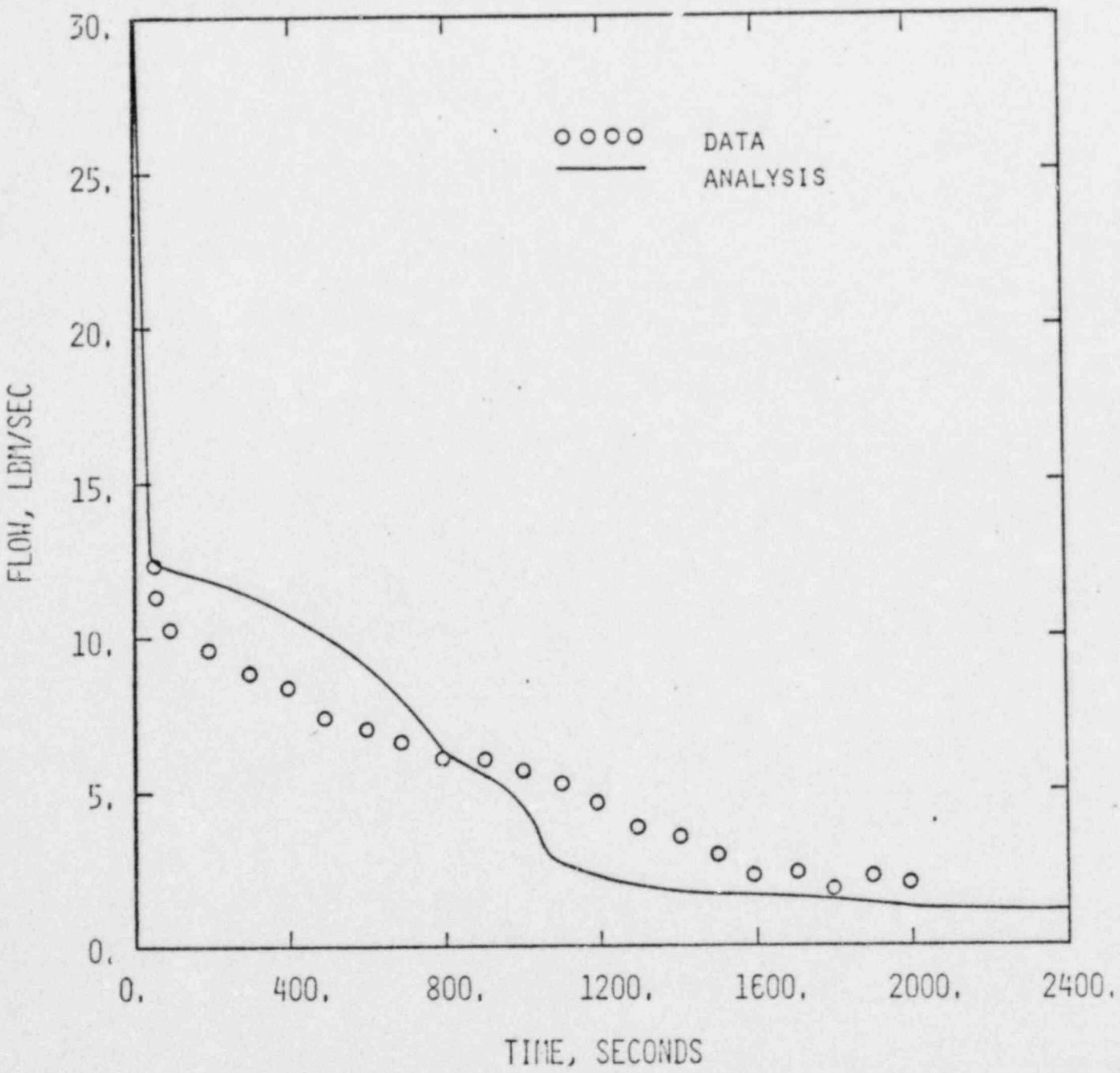

FIGURE 3-6

LOFT L3-6 BLIND ANALYSIS
PRIMARY SYSTEM MASS INVENTORY

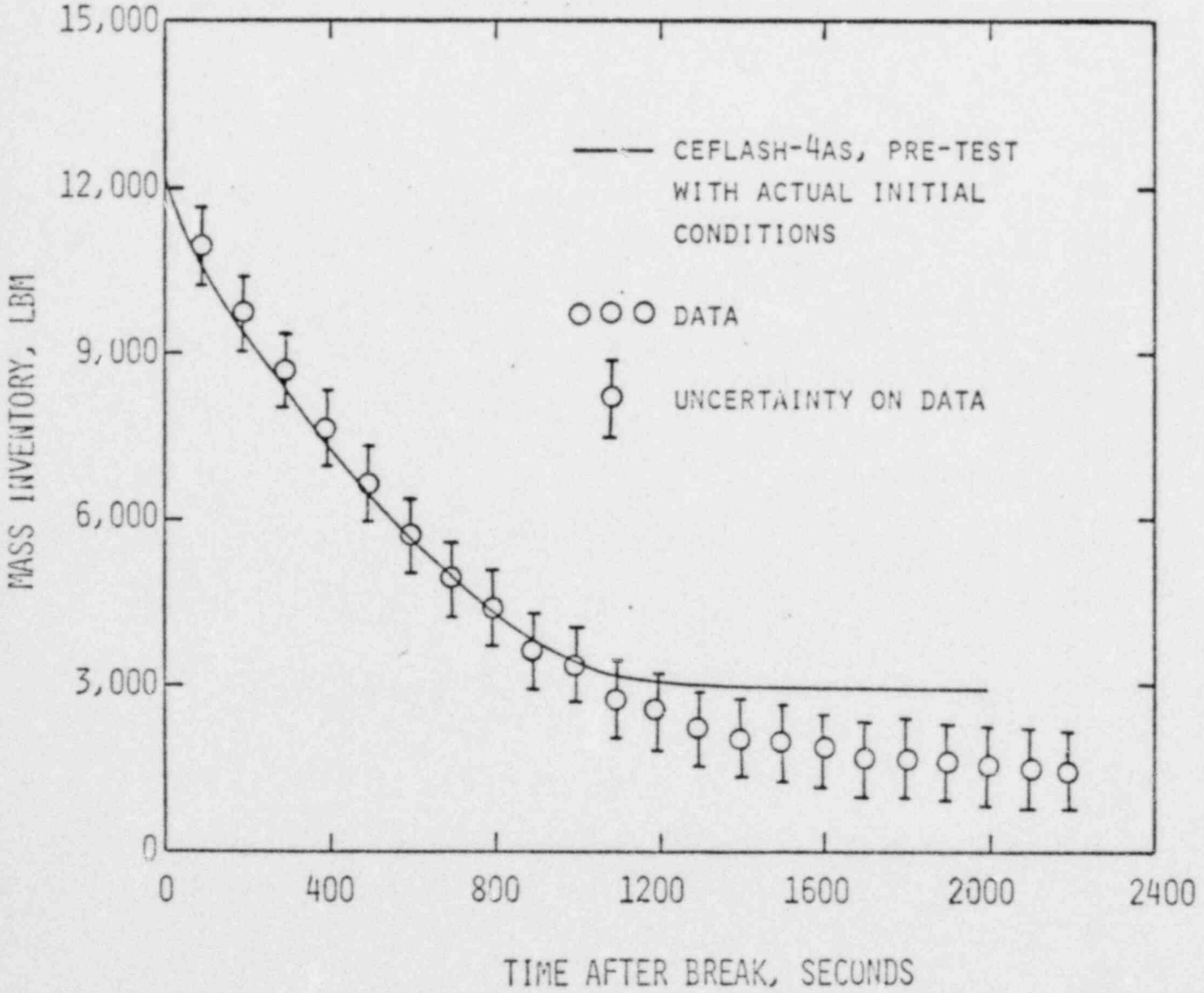

FIGURE 3-7

LOFT L3-6 BLIND ANALYSIS
PRESSURE DROP ACROSS PRIMARY COOLANT PUMPS

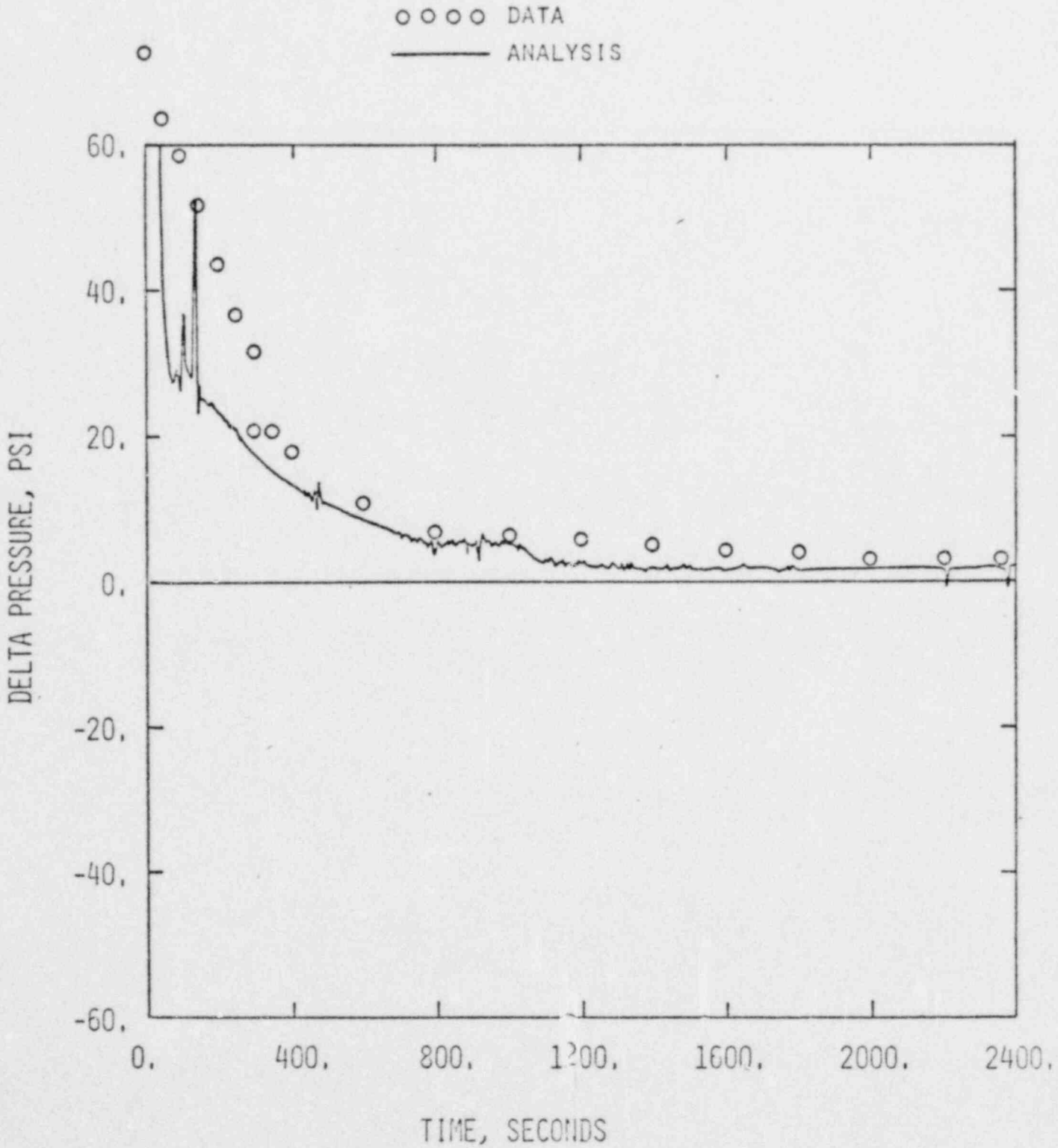

FIGURE 3-8

LOFT L3-6 BLIND ANALYSIS
SECONDARY SIDE PRESSURE

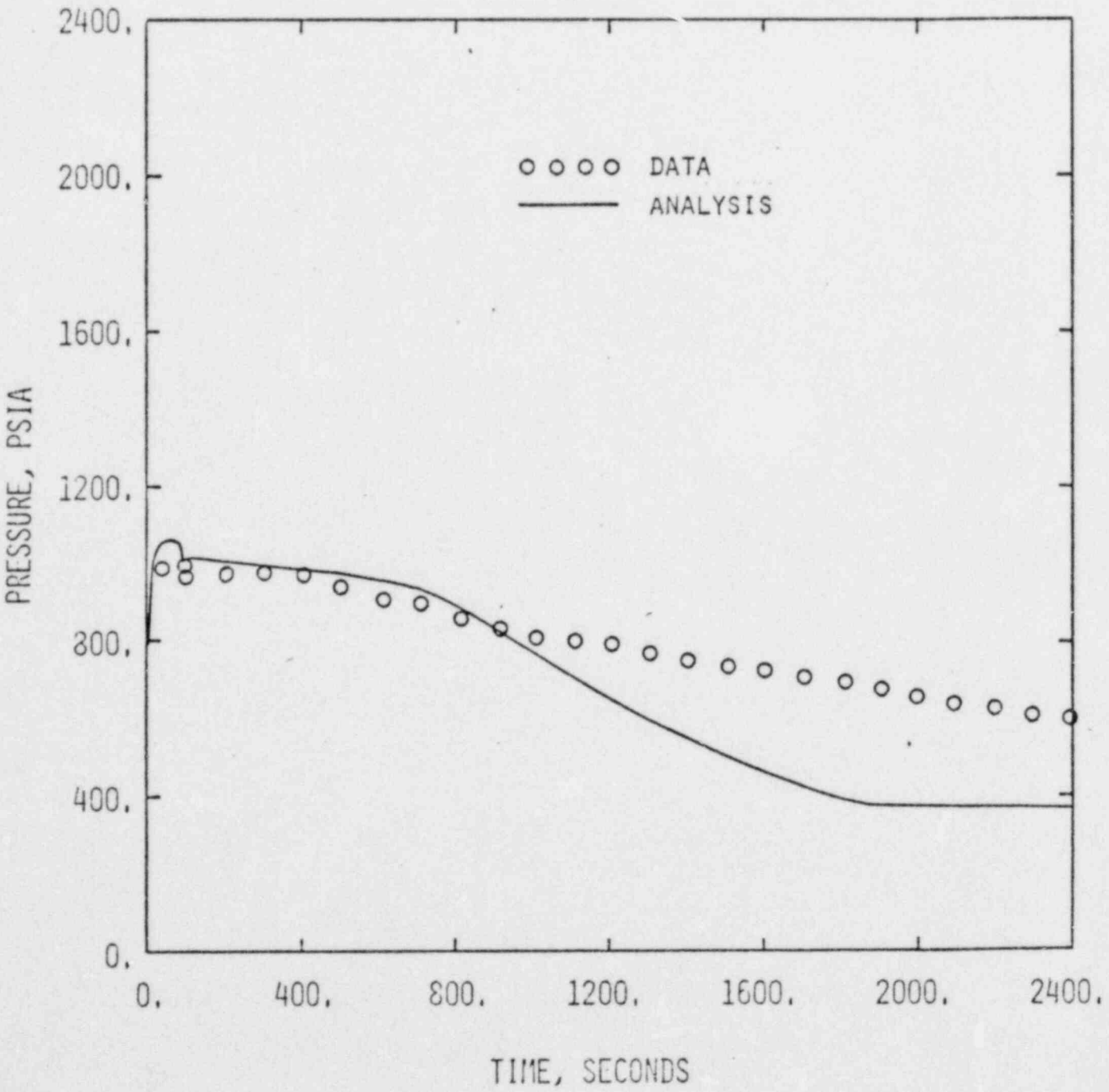

FIGURE 3-9

LOFT L3-6 BLIND ANALYSIS
INNER VESSEL MIXTURE LEVEL

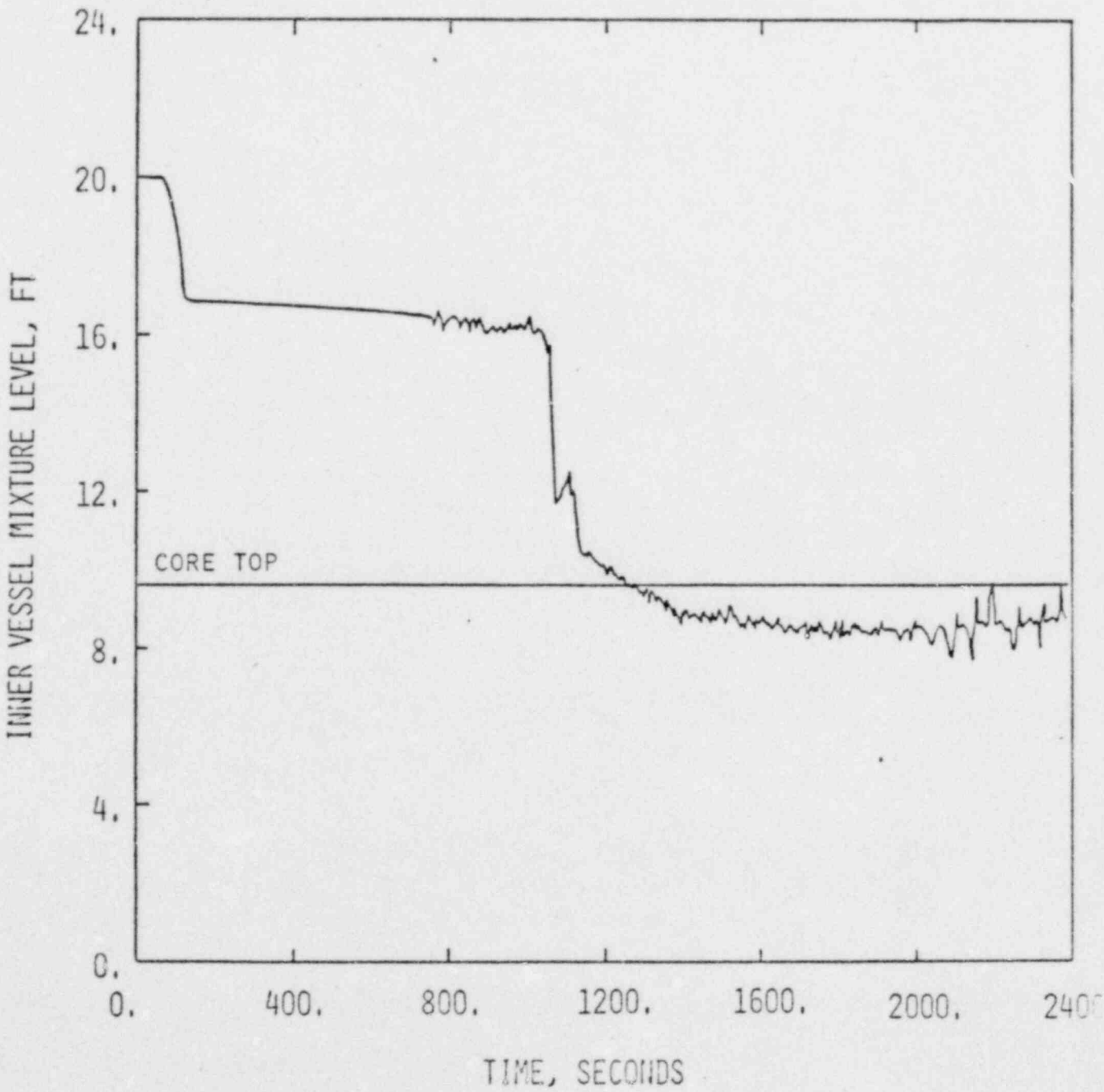

FIGURE 3-10

LOFT L3-6 POST-TEST ANALYSIS
BREAK FLOW QUALITY ENHANCEMENT

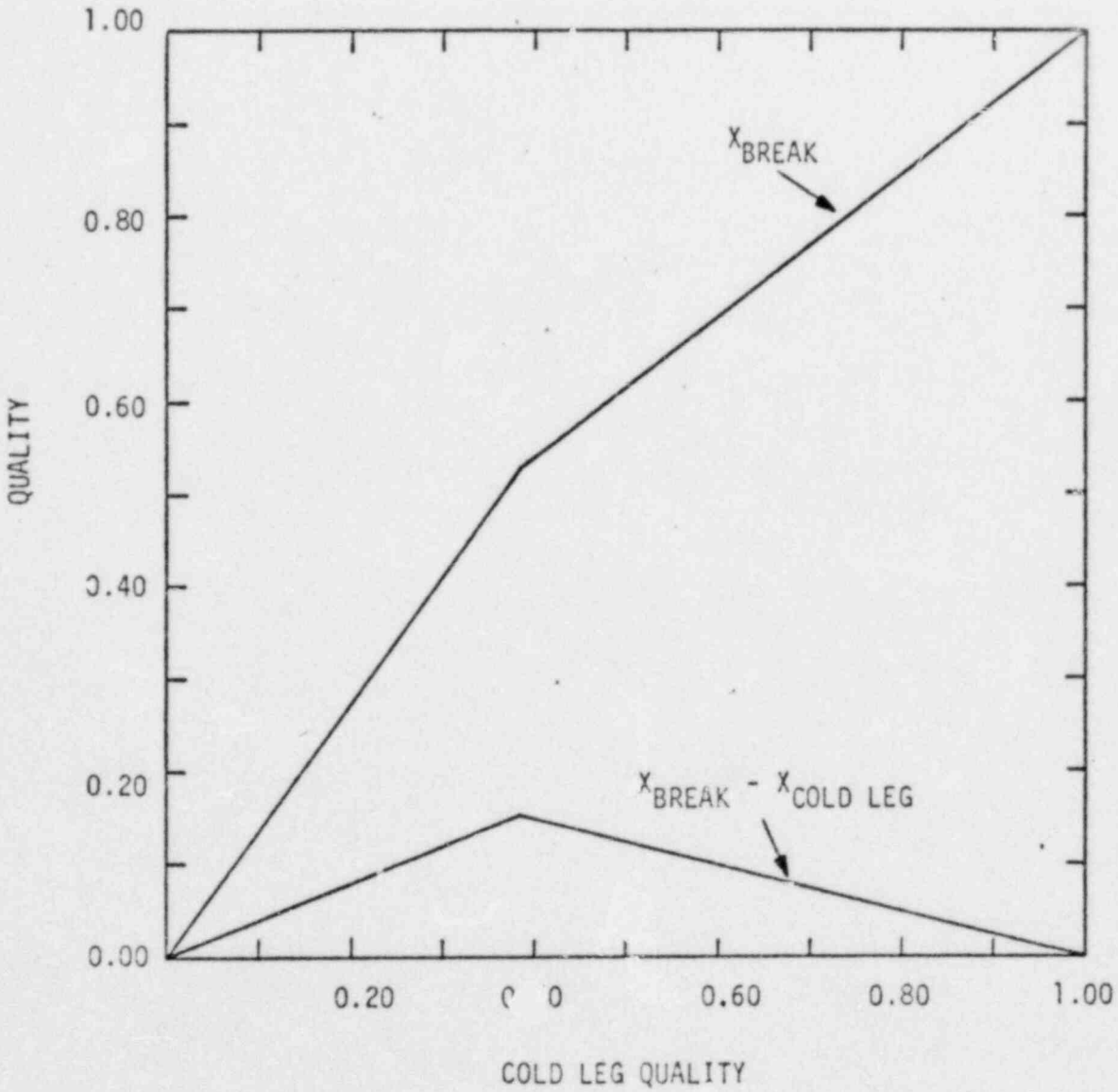

FIGURE 3-11

LOFT L3-6 POST-TEST ANALYSIS
PRIMARY SYSTEM PRESSURE

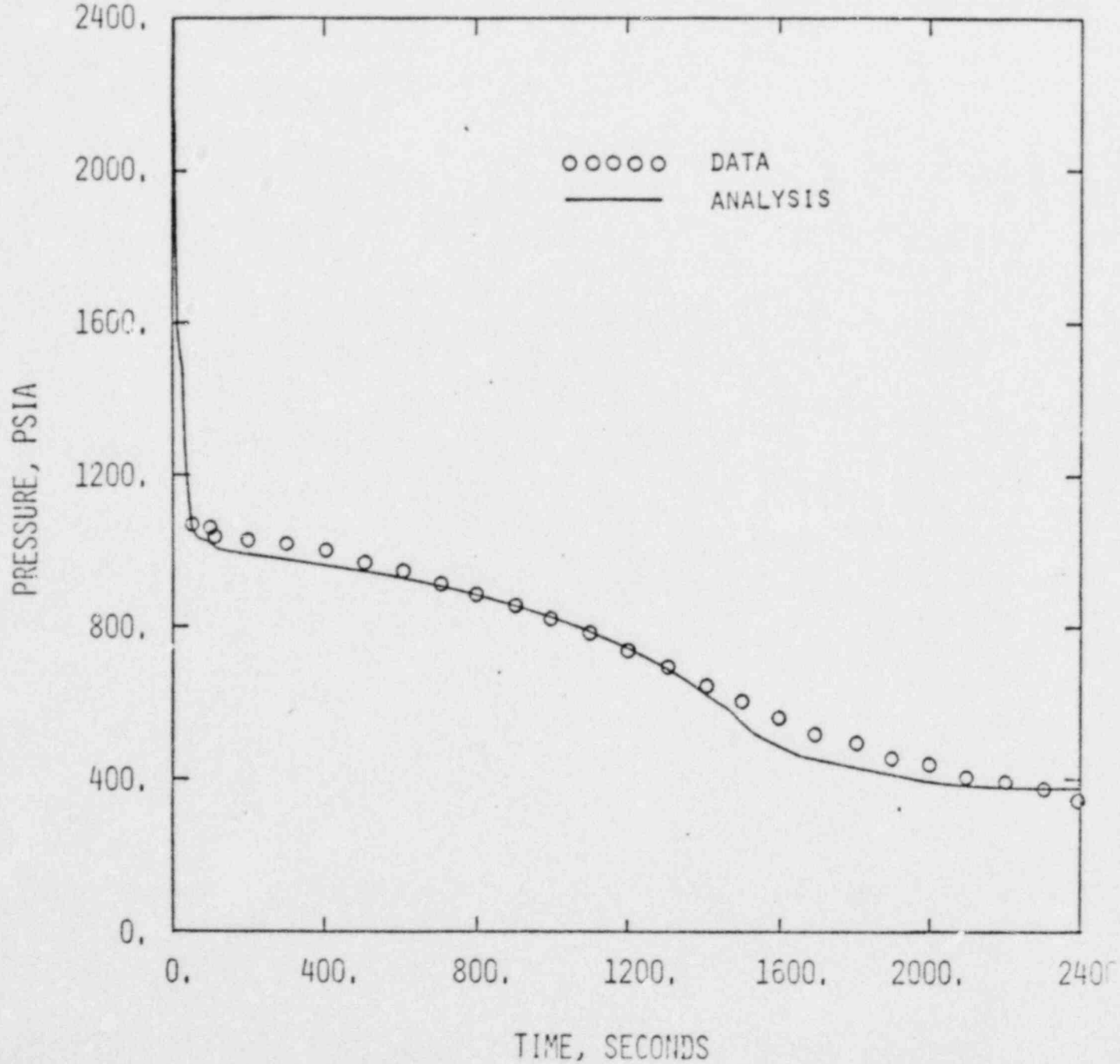

FIGURE 3-12

LOFT L3-6 POST-TEST ANALYSIS
INNER VESSEL MIXTURE LEVEL

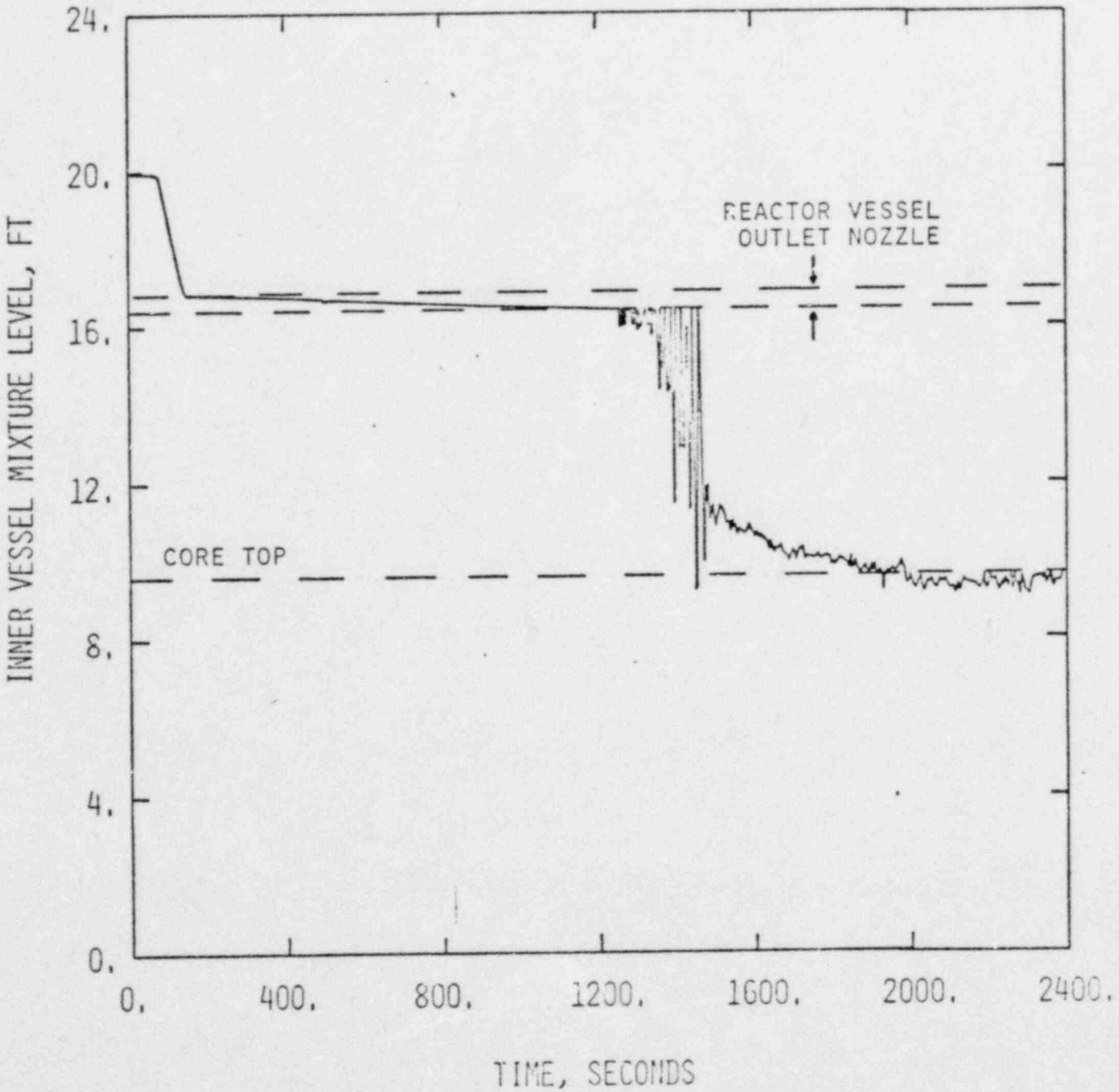

FIGURE 3-13

LOFT L3-6 POST-TEST ANALYSIS
PRESSURE DROP ACROSS PRIMARY COOLANT PUMPS

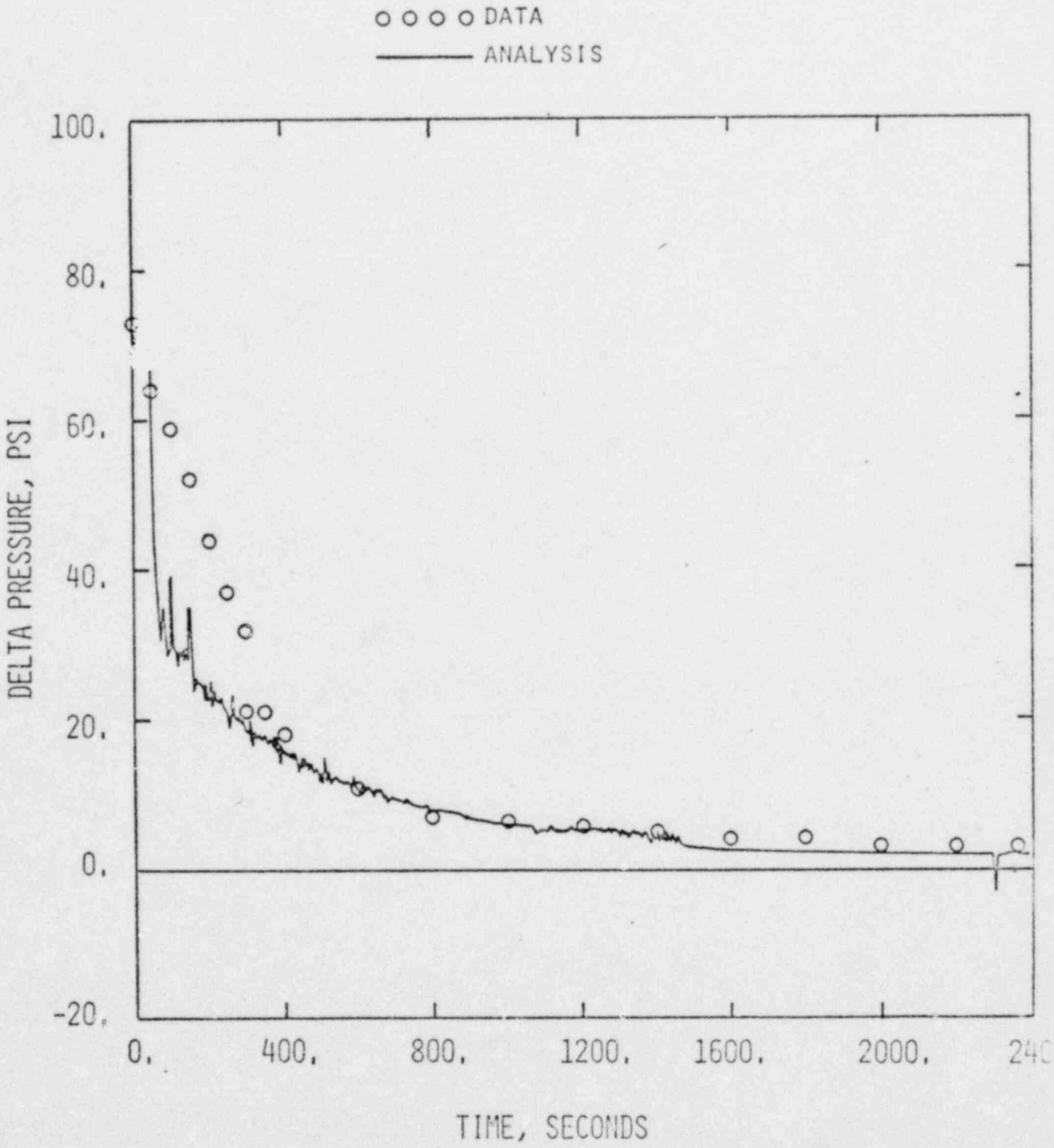

FIGURE 3-14

LOFT L3-6 POST-TEST ANALYSIS
SECONDARY SIDE PRESSURE

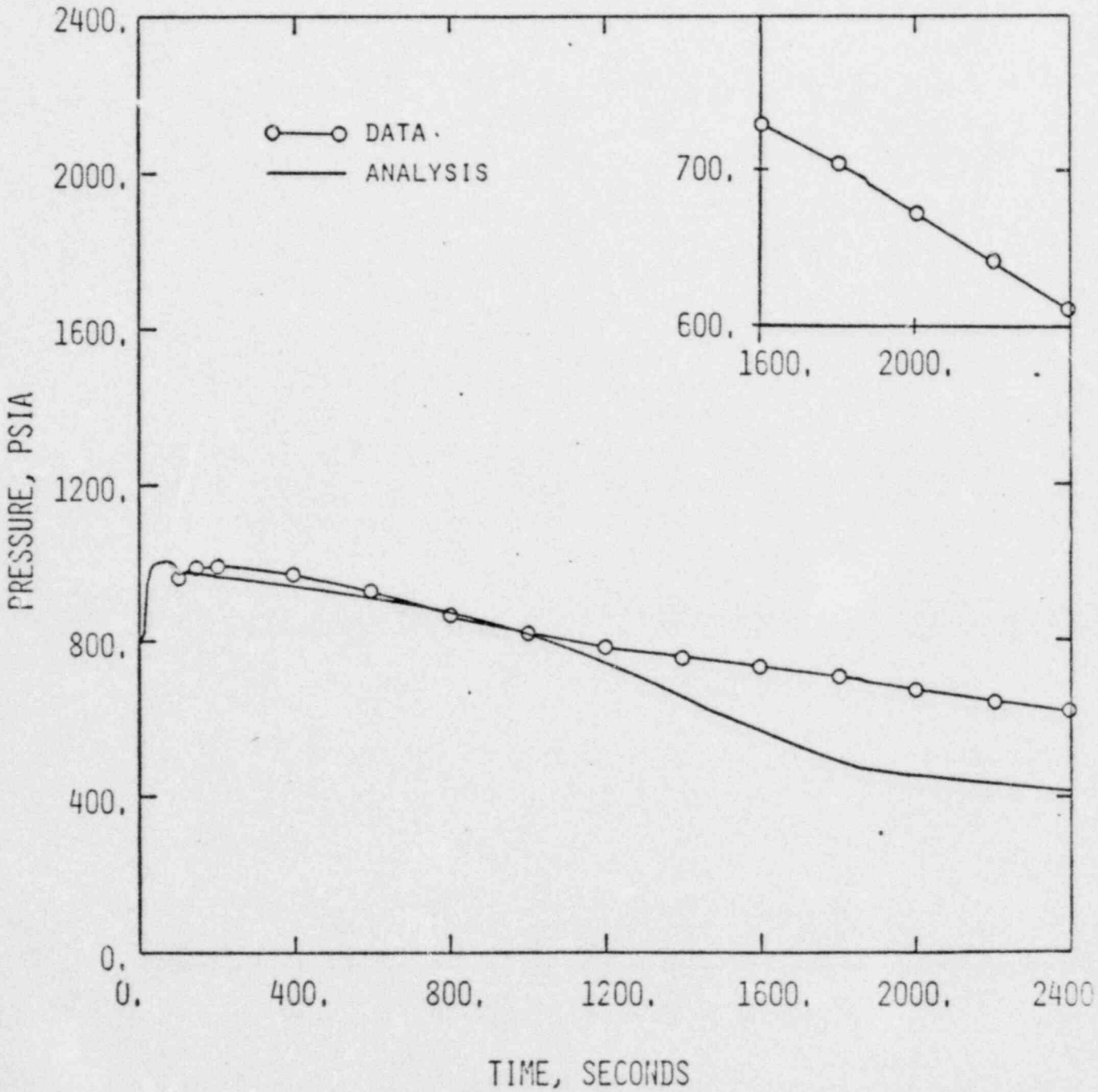

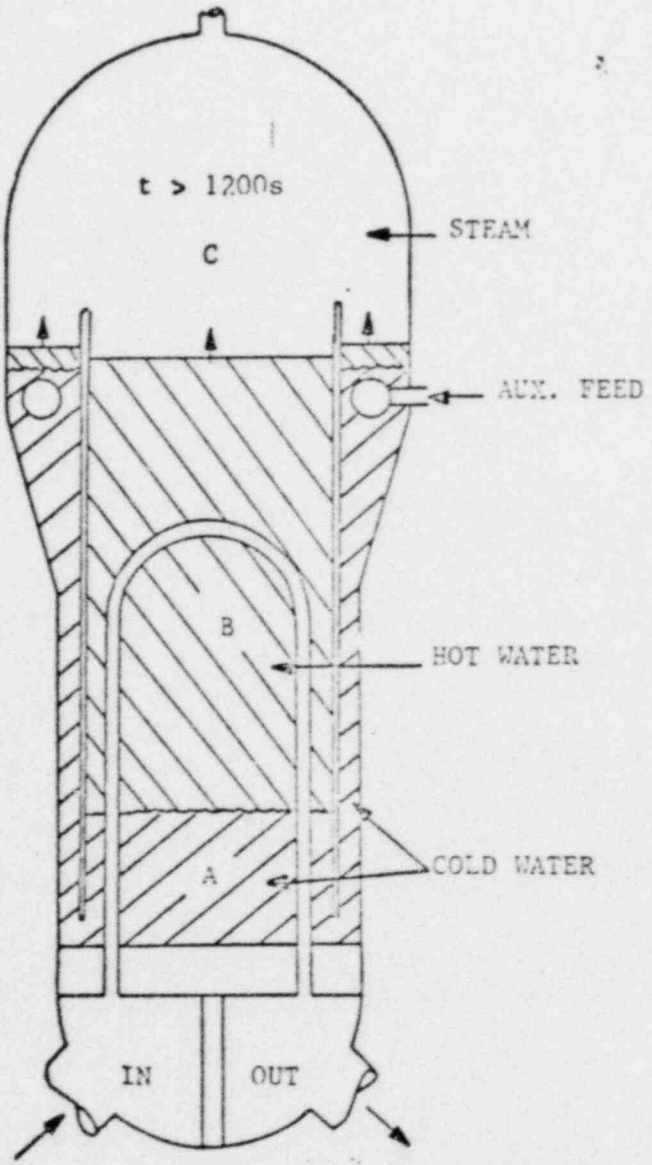

FIGURE 3-15

LOFT L3-6 STEAM GENERATOR
MIXED FOWARD/REVERSE HEAT TRANSFER MODE

FIGURE 3-16

LOFT L3-6 STEAM GENERATOR
TEMPERATURE TRANSIENTS
AND
SECONDARY SIDE LIQUID LEVEL ABOVE TUBE SHEET

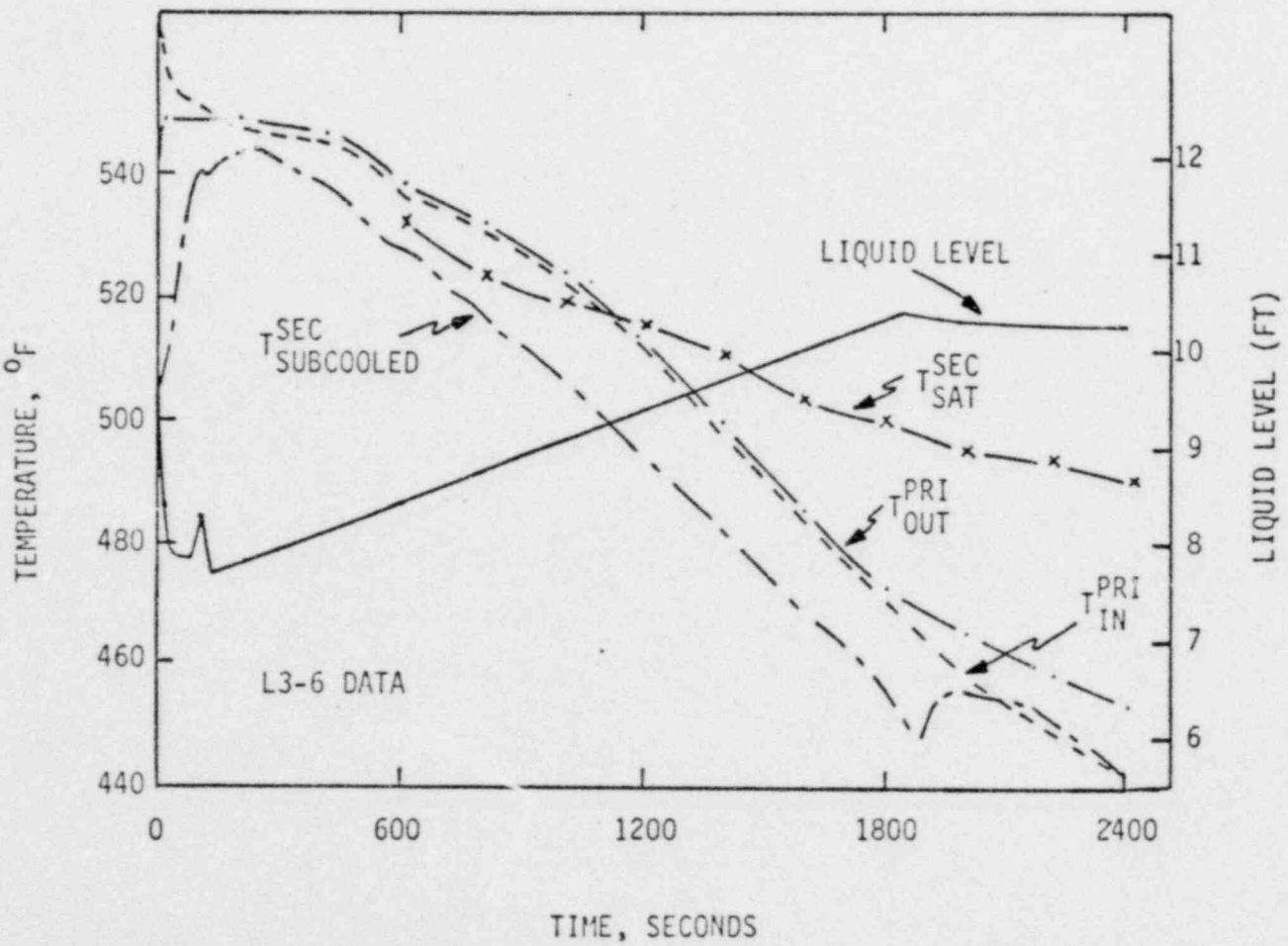

FIGURE 3-17

LOFT L3-6 POST-TEST ANALYSIS
BREAK FLOW

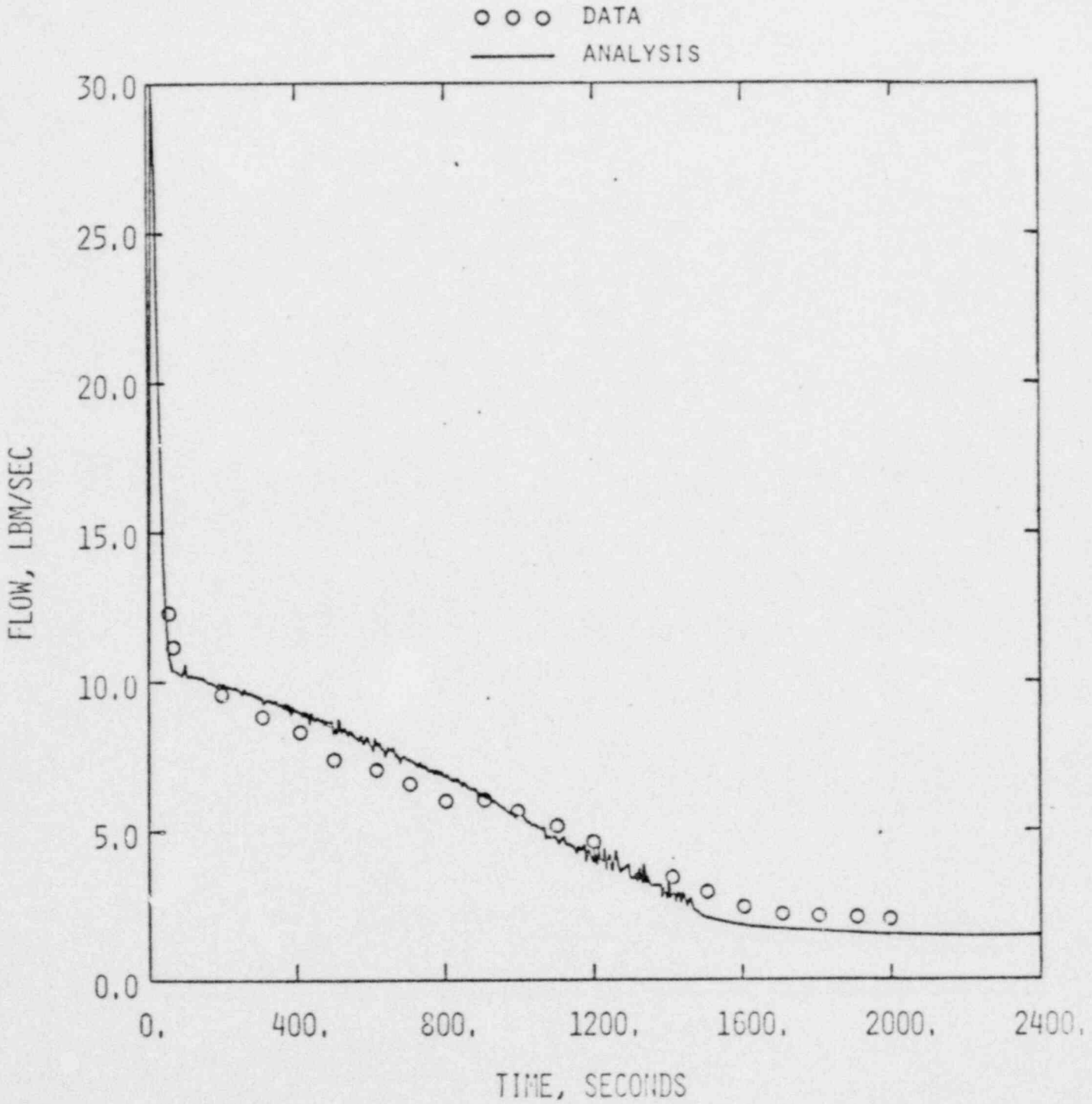

FIGURE 3-18

LOFT L3-6 POST-TEST ANALYSIS
PRIMARY SYSTEM MASS INVENTORY

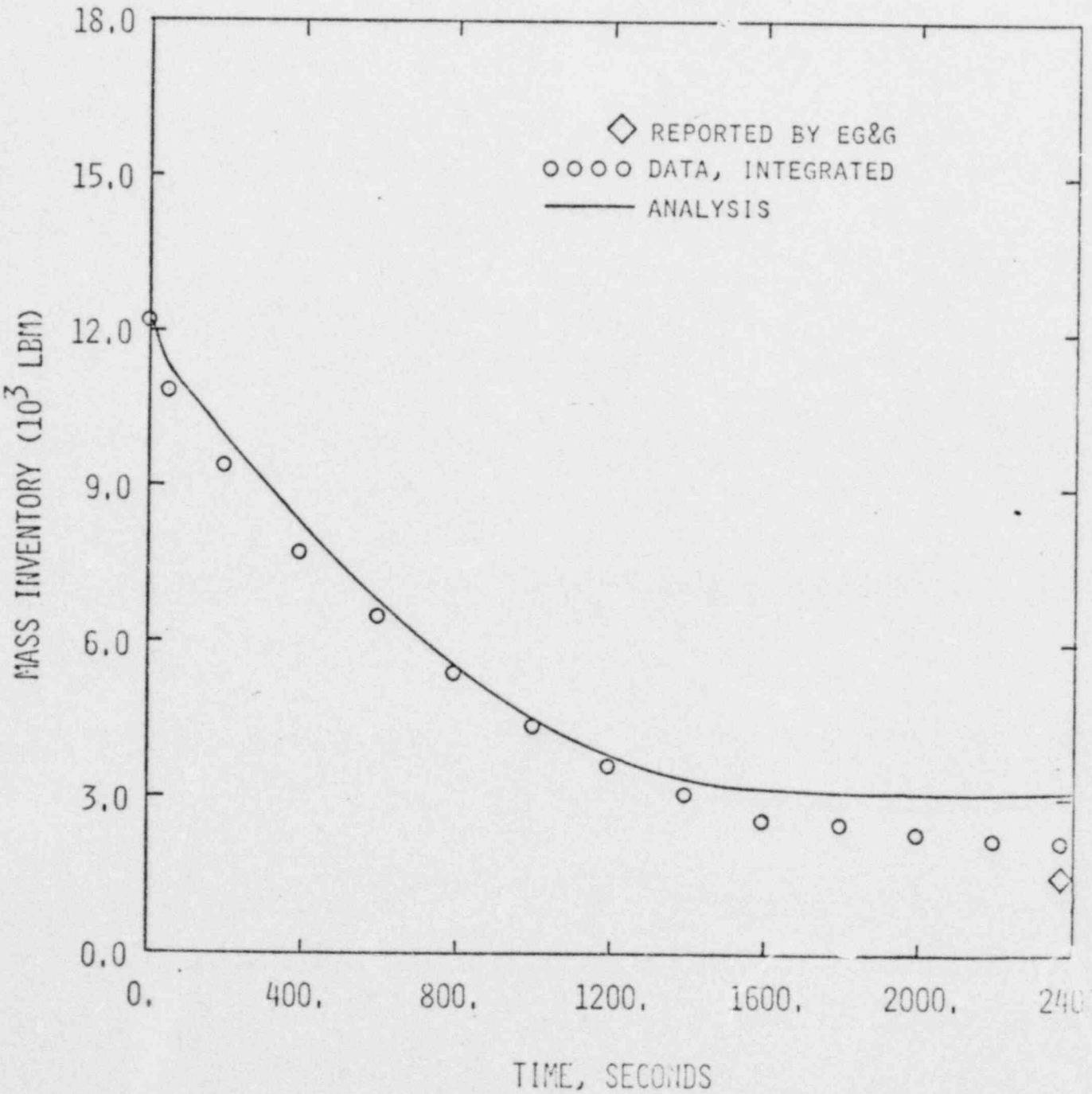

4.0 IMPACT ON PWR ANALYSIS

There are four aspects of the L3-6 analysis which could conceivably affect the analyses of commercial PWRs. They are:

1. The selection of 0.85 as a discharge coefficient on the critical flow correlation used for the L3-6 analysis.

2. The code modification used to model the wall heat (piping to coolant) which was used in the L3-6 analysis.

3. Modelling of the two-phase pump head degradation behavior.

4. Equilibrium modelling of fluid conditions in the steam generator secondary side.

The impact of the items summarized above on the analysis of a commerical PWR is discussed in the following paragraphs.

4.1 DISCHARGE COEFFICIENT/BREAK FLOW MODEL

The C-E analysis of LOFT Test L3-6 modeled the simulated break using the Homogeneous Equilibrium Model (HEM) for critical flow. This model was used since it best represents two-phase flow through break nozzles in experiments. In addition to using the HEM for critical flow calculations, two other models were used. A discharge coefficient of 0.85 was found to predict this test data better than a discharge coefficient of 1.0, and the quality of the primary coolant leaving the system was higher than the quality in the cold leg node (pump discharge piping), see Section 3.4.2.3 for details. The effect of these modeling choices for the L3-6 analysis is as follows:

1. The adjustment of the break quality with respect to the cold leg quality, had a small effect on the overall system behavior (Figure 4-1).

2. The blind analysis of LOFT Test L3-6 used HEM critical flow with a discharge coefficient of unity. The post-test analysis, however, found that using an effective break area of 85% of the physical size of the leak predicted the LOFT system behavior for L3-6. The effect of varying the effective break size is shown in Figure 4-2. The CEN-115 model is used to analyze a spectrum of break sizes. This yields the same results as varying the discharge coefficient.

The effect of break flow model used for the L3-6 analysis would be covered by the break spectrum performed in licensing analyses. Therefore, the CEN-115 Model is not impacted by this aspect of the L3-6 analysis model.

4.2 PIPING TO COOLANT HEAT TRANSFER

The piping to coolant wall heat model used for the CEN-115 analysis required modification in order to better model the LOFT system for Test L3-6. This modification was needed because wall heat for the LOFT facility is atypically high relative to a commerical PWR. This fact is verified by comparison of Figures 4-3 and 4-4. Figure 4-3 presents the integrated energy balance for LOFT Test L3-6. It shows that at 2000 seconds the piping to coolant heat input is about 50% of the core heat input. Figure 4-4 presents the same information for a typical C-E (System 80) reactor. It shows that piping to coolant heat input for a PWR is only about 1% of the core heat input.

Wall heat, therefore, has a negligible effect on the analysis of a PWR. Consequently, the modification to the wall heat model for LOFT Test L3-6 has no impact on the CEN-115 Model.

4.3 TWO-PHASE PUMP HEAD DEGRADATION

The C-E analysis of LOFT Test L3-6 used a two-phase pump head degradation multiplier which is based on pump tests performed by the Aerojet Nuclear

Corporation (Reference 4-1). This is the same model which is used in the CEN-115 analysis for C-E PWRs. In the post-test analysis of LOFT Test L3-6, a two-phase pump degradation multiplier, based on C-E/EPRI pump performance tests (Reference 4-2) was examined to determine the effect of its use on the system behavior. The two models are shown in Figure 4-5. Comparison between L3-6 analyses with the ANC model and the C-E/EPRI model indicates that there is a marginal improvement of the comparison between the calculated pump head and the data when using the C-E/EPRI model (Figure 4-6). However, the use of a different head degradation model has negligible effect on the overall system behavior (Figure 4-7).

It is therefore concluded that the two-phase pump head degradation model has little effect on the system behavior and that no change to the CEN-115 Model is required.

4.4 NON-EQUILIBRIUM CONDITIONS IN THE SECONDARY SIDE

It was determined in the post-test analysis that non-equilibrium conditions existed on the secondary side during LOFT Test L3-6. The result of this condition was a decrease in the heat transfer from the secondary to the primary. That is, the layer of subcooled fluid below the saturated water on the secondary side provides less of a heat source for the primary side compared to when the secondary side is modeled using a thermal equilibrium approach.

In the CEN-115 Model, the secondary side is modeled as an equilibrium control volume. This modeling choice tends to maximize heat transfer into the primary system since the secondary side is at saturated conditions. Figure 4-8 graphically shows the effect of using an equilibrium versus a non-equilibrium treatment. The top plot shows the CEFLASH-4AS treatment. The primary fluid enters the steam generator at the saturation temperature of the primary side. It is then heated up to approximately the secondary temperature. For the FLASH treatment heat is always added to the primary system. This is conservative since it tends to keep the primary pressure higher thus reducing the amount of ECC injection. In the lower plot of Figure 4-8, the non-equilibrium condition is depicted. (Note that this information was taken from actual test data). The primary side fluid enters

the steam generator at the saturation temperature of the primary side. Primary to secondary heat transfer takes place in the subcooled portion of the steam generator. The primary fluid is then heated by the portion of the tubes which is covered with saturated water. It is then cooled by the subcooled layer before exiting the steam generator. The result of this is less net heat transfer from the secondary to the primary than would be obtained with an equilibrium treatment.

Therefore, it is concluded that use of an equilibrium model in the CEFLASH-4AS code or the secondary yields slightly conservative results compared to the actual non-equilibrium conditions. No modifications to the C-E model used for the CEN-115 analysis are considered necessary to model non-equilibrium conditions on the secondary side of the steam generator.

4.5 CONCLUSIONS

A review of the modeling changes which were made for the best-estimate analysis of LOFT L3-6 indicates that the changes were made to better represent the LOFT facility only and have no impact on the model used to analyze PWR small break LOCAs. Therefore, no changes are anticipated to the C-E Small Break Model used for CEN-115.

4.6 REFERENCES FOR SECTION 4.0

4-1 CENPD-137, "Calculative Methods for the C-E Small Break LOCA Evaluation Model", August, 1974.

CENPD-137, Supplement 1, "Small Break Model, Calculative Methods for the C-E Small Break LOCA Evaluation Model", January, 1977.

4-2 D. A. Kreps, "C-E/EPRI Two Phase Pump Performance Program", Technical paper for Fifth Water Reactor Safety Research Information Meeting, Gaithersburg, MD, November 7, 1977.

FIGURE 4-1

LOFT L3-6 PRIMARY SYSTEM PRESSURE
EFFECT OF BREAK QUALITY ENHANCEMENT

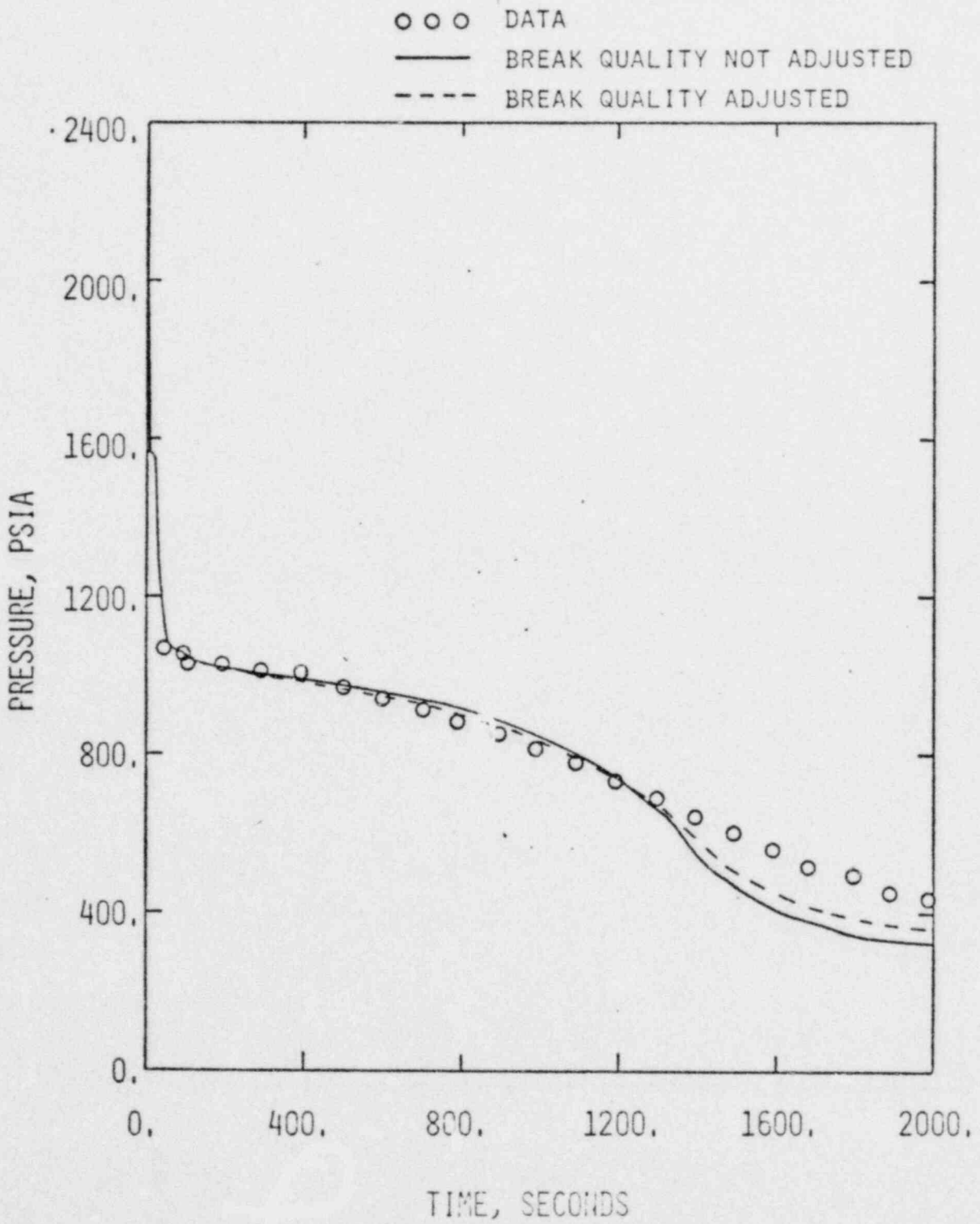

FIGURE 4-2

LOFT L3-6 PRIMARY SYSTEM PRESSURE
EFFECT OF BREAK DISCHARGE COEFFICIENT

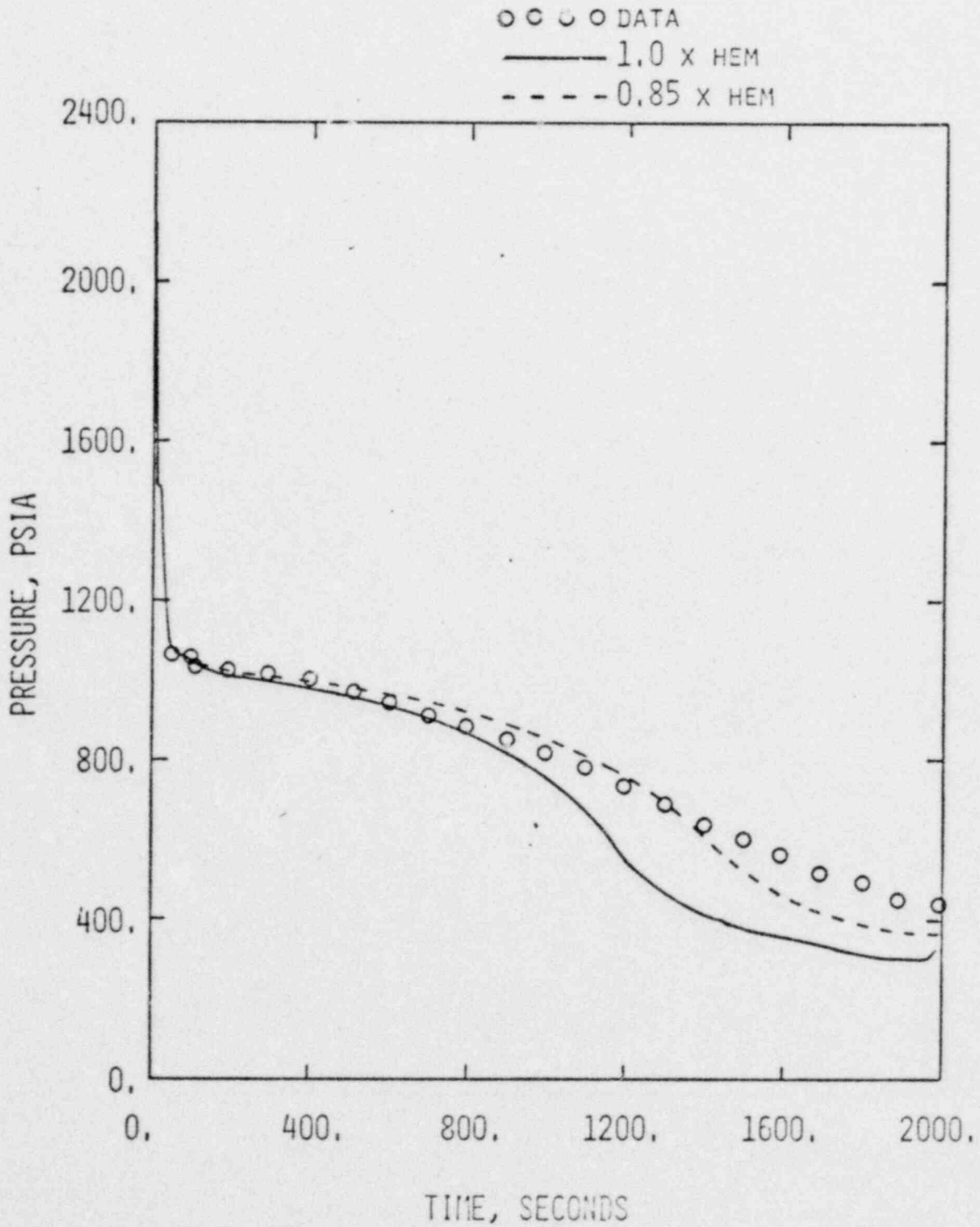

FIGURE 4-3

LOFT L3-6 PRIMARY SYSTEM ENERGY BALANCE

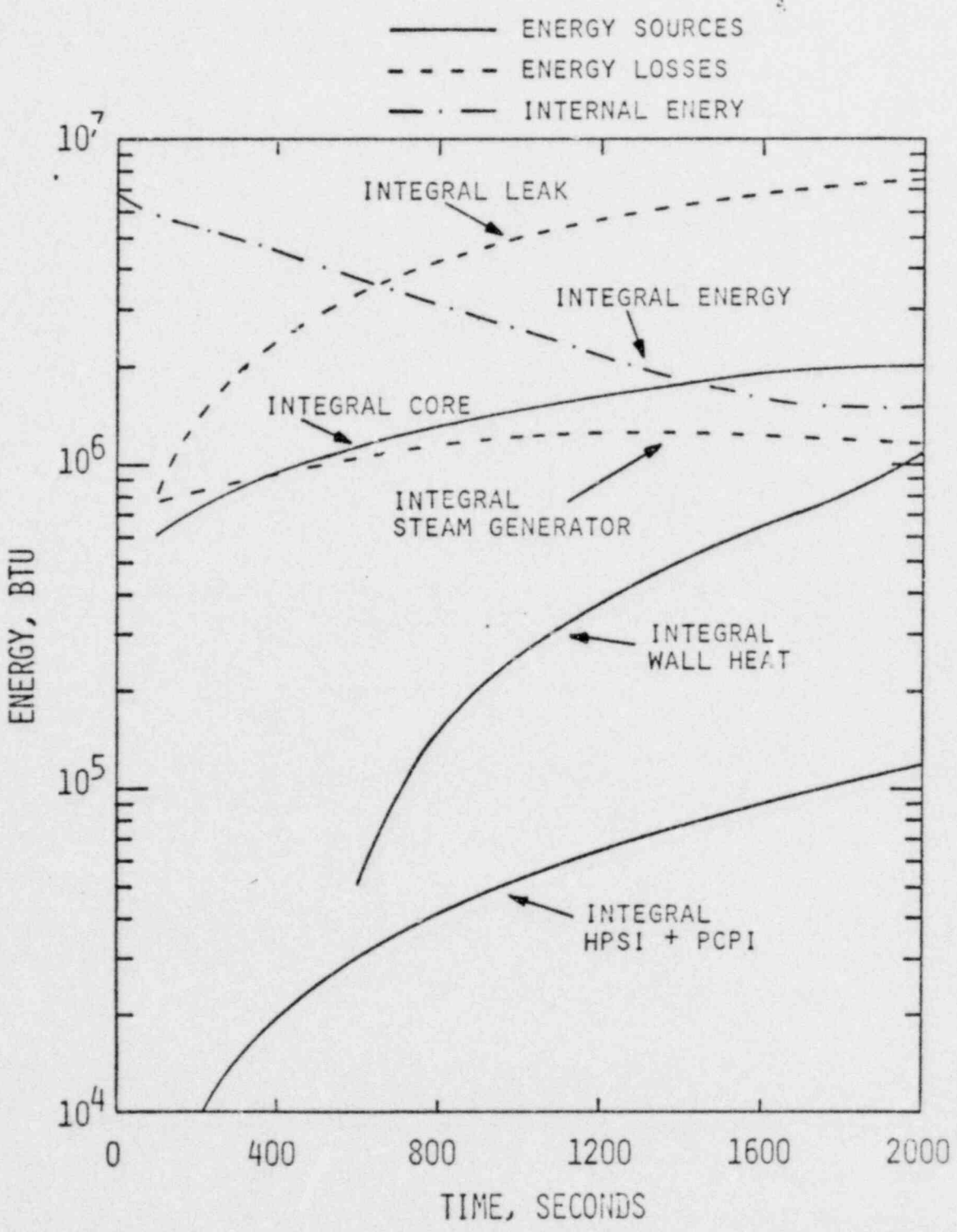

FIGURE 4-4

C-E PWR

PRIMARY SYSTEM ENERGY BALANCE

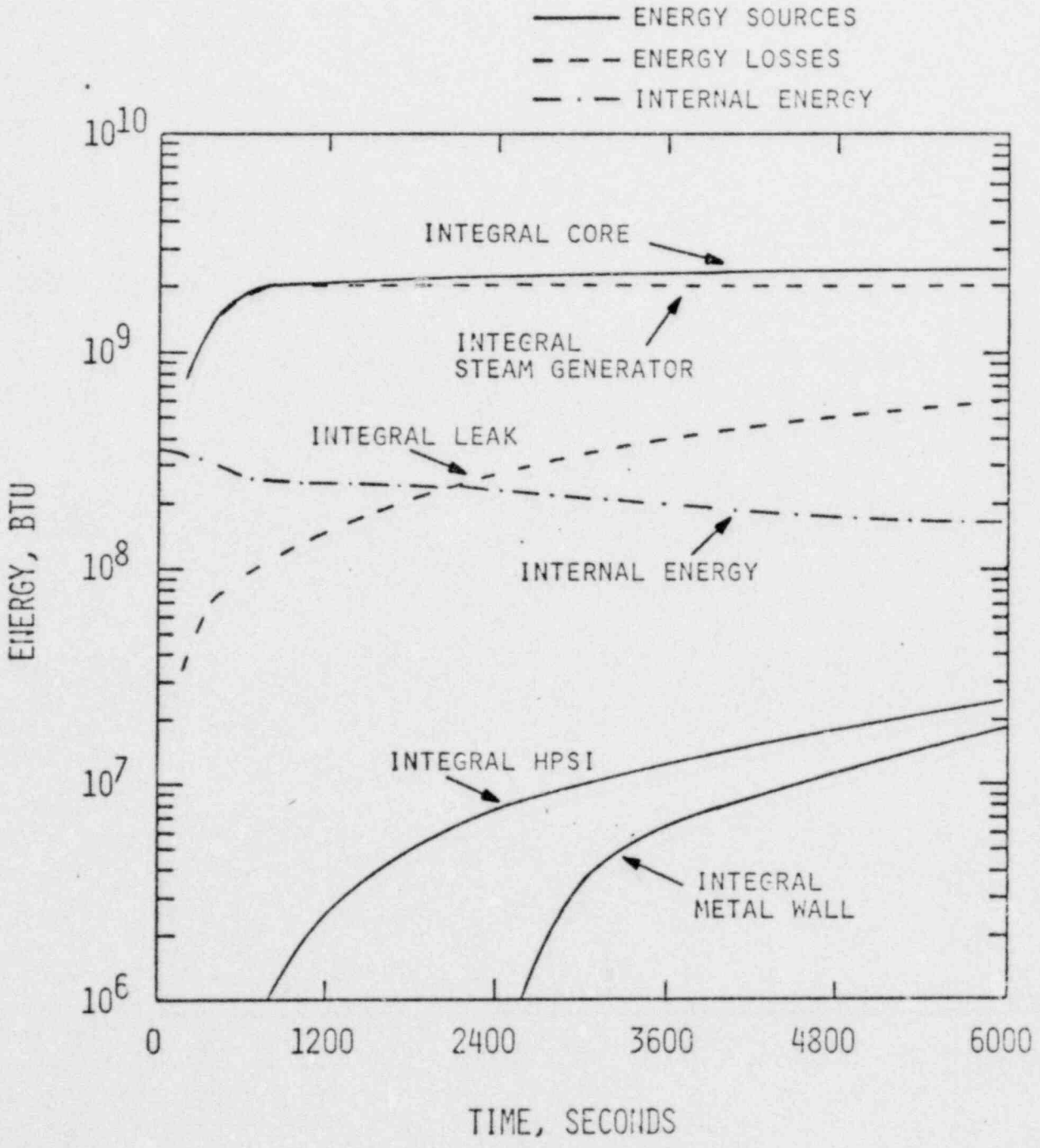

FIGURE 4-5

TWO-PHASE HEAD DEGRADATION COEFFICIENT

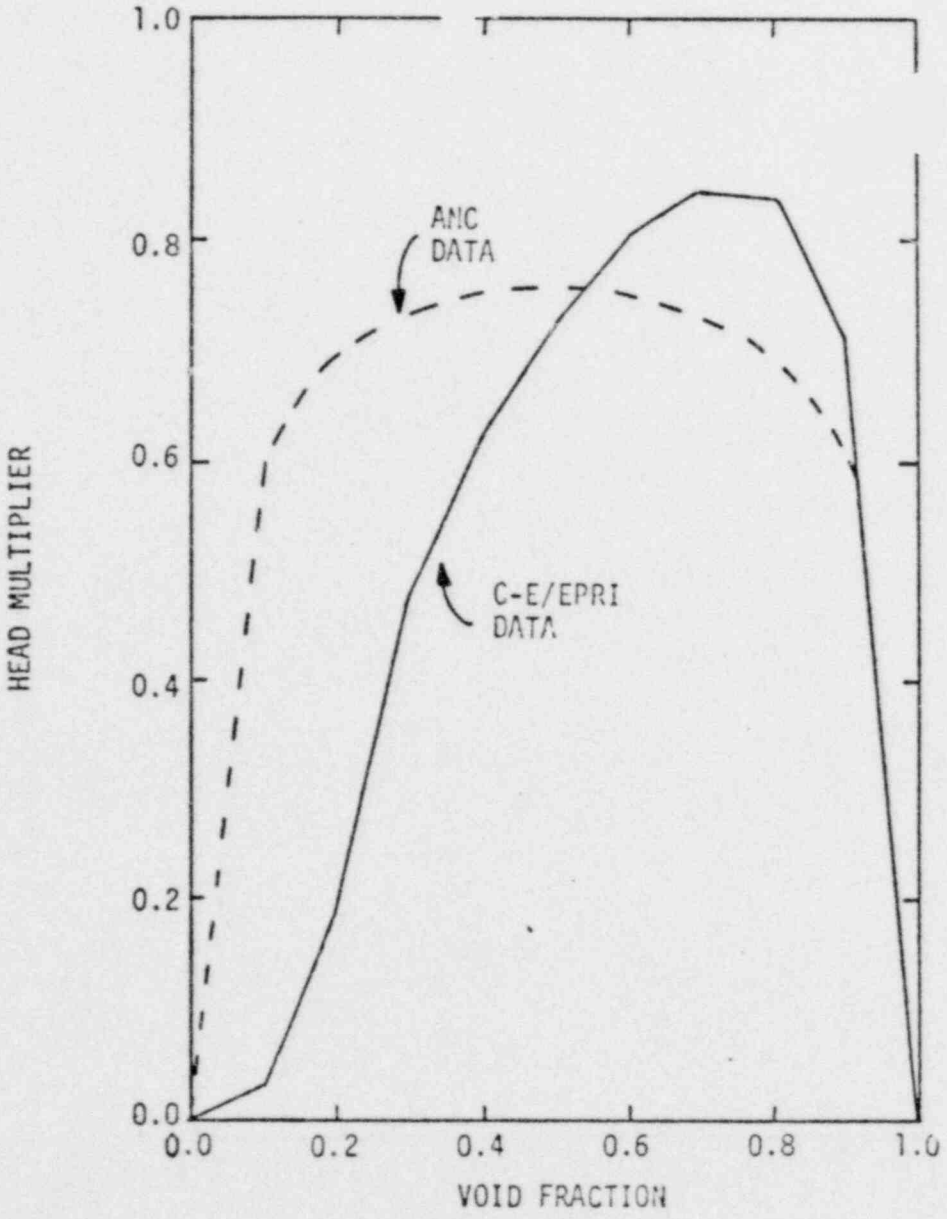

FIGURE 4-6

LOFT L3-6 PRESSURE DROP ACROSS PRIMARY COOLANT PUMPS
EFFECT OF TWO-PHASE HEAD DEGRADATION COEFFICIENT

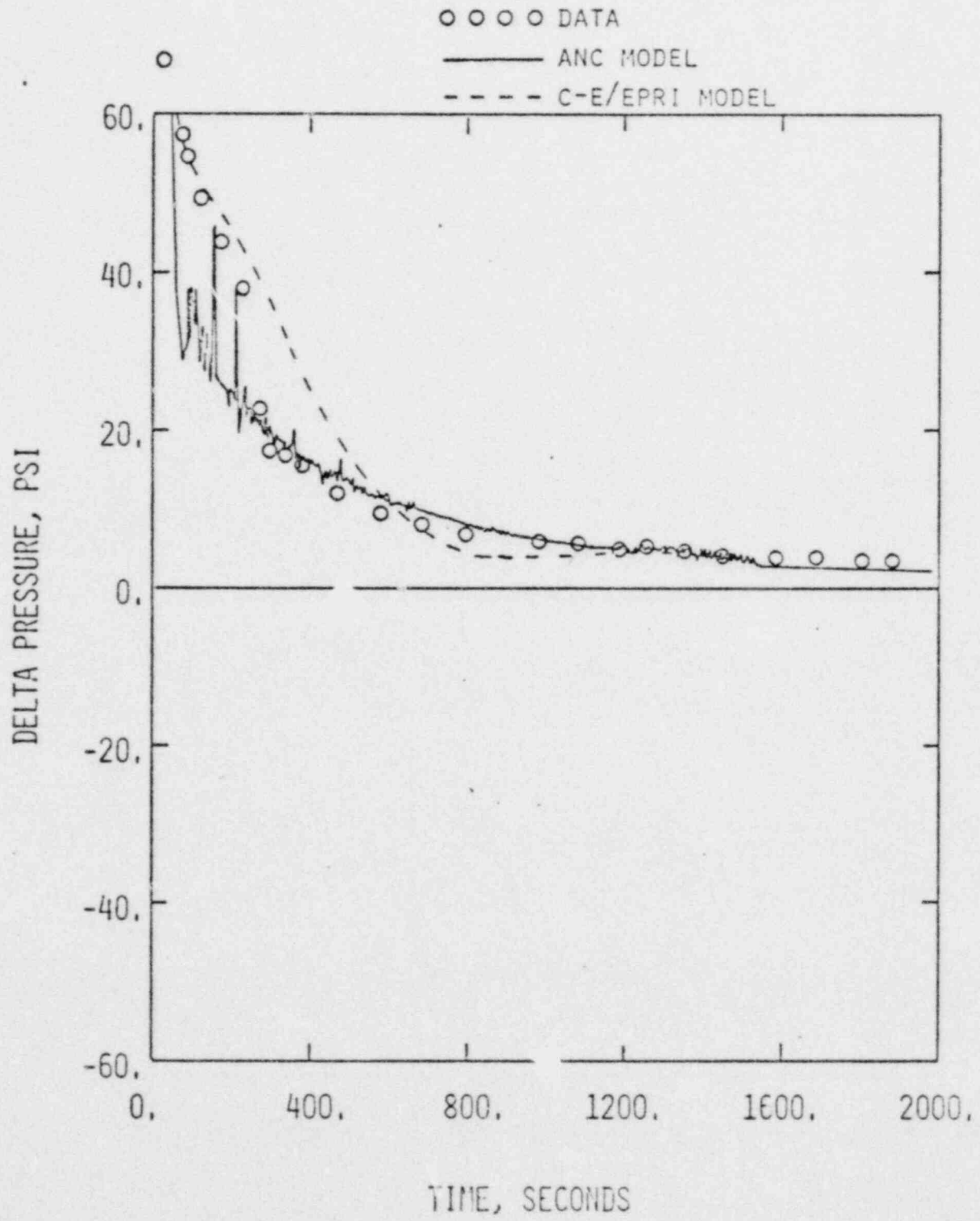

FIGURE 4-7

LOFT L3-6 PRIMARY SYSTEM PRESSURE
EFFECT OF TWO-PHASE HEAD DEGRADATION COEFFICIENT

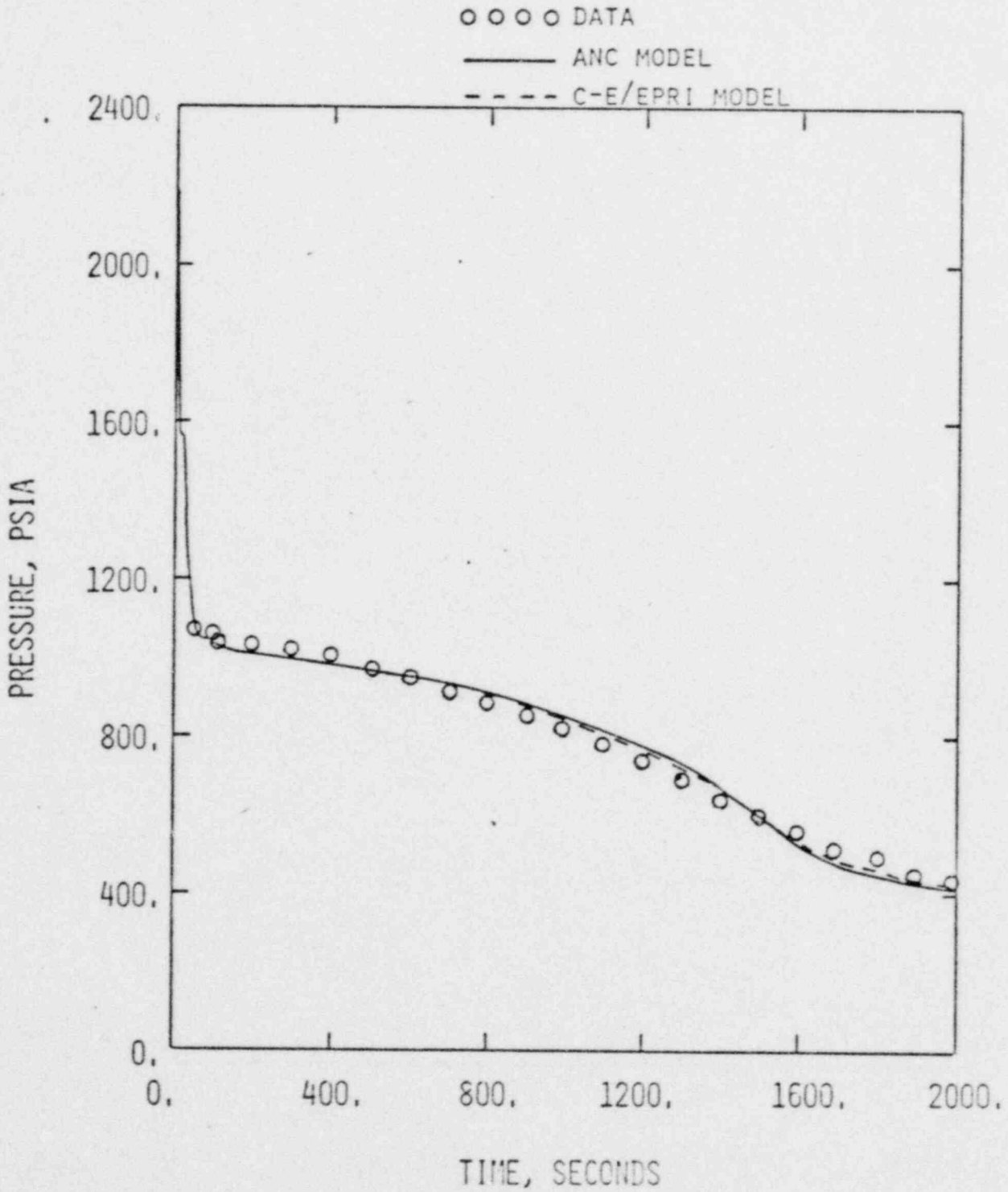

5.0 CONCLUSIONS

This report has presented the blind analysis and open post-test analysis for LOFT Test L3-6 as performed by Combustion Engineering, Inc. for the C-E Owner's Group on Post-TMI Efforts. In addition, the impact of the results of the analysis on PWR small break analyses has been evaluated. Based on the results of this report, the following conclusions are drawn.

1. The methods used by C-E for small break analyses adequately predict small break experiments.

2. The changes made to the pre-test model were required because of differences between anticipated versus actual initial conditions and operational procedures or because of atypicalities of the LOFT facility.

3. The changes to the CEN-115 Model for LOFT Test L3-6 are either covered by current licensing analysis practices (i.e. break spectrum) or have little impact on the analysis of large PWR's (e.g. wall heat).